Published Online: 28 Oct 2009

Process Systems Engineering

Model predictive control with learning-type set-point: Application to artificial pancreatic β-cell

Youqing Wang [1 2 3], Howard Zisser [1 3], Eyal Dassau [1 2 3], Lois Jovanovič [1 2 3], Francis J. Doyle III [1 2 3 *]

[1]Dept. of Chemical Engineering, University of California, Santa Barbara, CA 93106

[2]Biomolecular Science & Engineering Program, University of California, Santa Barbara, CA 93106

[3]Sansum Diabetes Research Institute, Santa Barbara, CA 93105

email: Francis J. Doyle (frank.doyle@icb.ucsb.edu)

[*]Correspondence to Francis J. Doyle III, Dept. of Chemical Engineering, University of California, Santa Barbara, CA 93106

Funded by:

- Juvenile Diabetes Research Foundation (JDRF); Grant Number: Grant # 22-2007-1801
- Otis Williams Fund at the Santa Barbara Foundation

KEYWORDS

model predictive control • iterative learning control (ILC) • indirect ILC • artificial pancreatic β-cell • Type 1 diabetes mellitus

ABSTRACT

A novel combination of model predictive control (MPC) and iterative learning control (ILC), referred to learning-type MPC (L-MPC), is proposed for closed-loop control in an artificial pancreatic β-cell. The main motivation for L-MPC is the repetitive nature of glucose-meal-insulin dynamics over a 24-h period. L-MPC learns from an individual's lifestyle, inducing the control performance to improve from day to day. The proposed method is first tested on the Adult Average subject presented in the UVa/Padova diabetes simulator. After 20 days, the blood glucose concentrations can be kept within 68-145 mg/dl when the meals are repetitive. L-MPC can produce superior control performance compared with that achieved under MPC. In addition, L-MPC is robust to random variations in meal sizes within ±75% of the nominal value or meal timings within ±60 min. Furthermore, the robustness of L-MPC to subject variability is validated on Adults 1-10 in the UVa/Padova simulator. © 2009 American Institute of Chemical Engineers AIChE J, 2010

Received: 12 February 2009; Revised: 25 August 2009

DIGITAL OBJECT IDENTIFIER (DOI)

10.1002/aic.12081 About DOI

ARTICLE TEXT

Introduction

Output regulation is a fundamental issue in control design.[1] For output regulation issue, the control objective is to make the outputs approach a given target Y_r as closely as possible. To achieve the control objective, a command is required to tell the controller what to do, and this command is named set-point. In most cases, the set-point is chosen to be the same as the target Y_r. Logically, this leads to the question of whether the target is the best choice for the set-point.

This prompts an additional question: what is the optimal set-point, and how can it be determined? If a process exhibits a repetitive behavior, e.g., batch processes and periodic continuous processes-iterative learning control (ILC) could be used to update the set-point and search for the optimal one. Therefore, there are two loops in the closed-loop system, as shown in Figure 1: a local controller is used to stabilize the system and regulate the outputs; an ILC is used to optimize the set-point for the local controller.

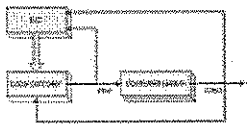

Figure 1. Block diagram of indirect iterative learning control.The narrow arrow lines denote the measurement information; the wide arrow line denotes the management decision. [Color figure can be viewed in the online issue, which is available at www.interscience.wiley.com.] [Normal View 13K | Magnified View 31K]

Generally speaking, there are two ways to use ILC: (1) it is utilized to determine the control signal directly, a method which is called direct ILC[2]; (2) it is used to update some parameters for the local controller, a method which is named indirect ILC.[2] According to this classification method, the algorithm proposed in this work is considered an indirect ILC algorithm. In a recent survey,[2] 207 articles from the Web of Science that featured "iterative learning control" in the title were reviewed, and only 16 of them were deemed to focus on indirect ILC. For indirect ILC, two essential issues need to be established: what algorithms are used to design the local control, and which parameters of the local controller are updated by ILC. Among the 16 indirect-ILC-related articles mentioned previously, ILC was used to update the set-point for the local control in only two works.[3][4] In the first study,[3] ILC was used to update the set-point for a PID controller, and then a standard PID with adaptive gain was used to replace the ILC-based PID. In the other work,[4] an anticipatory-type ILC (A-ILC) was used to adjust the set-point for a PID controller, and the proposed scheme was implemented on an X-Y platform.

In the present work, the local control is chosen as model predictive control (MPC) because of its superior abilities in dealing with multivariate processes, constraints, and nonlinearities. Furthermore, the ILC method proposed in this article is much easier to use and more intuitive than that used in the aforementioned references. In this novel combination, MPC is applied to the system and ILC is used to optimize the set-point for MPC. Hence, the proposed algorithm is denoted L-MPC. It should be pointed out that ILC and MPC have long been used together, in combinations such as BMPC,[5] 2D-GPILC,[6] and MPILC.[7] However, in each of these, MPC was used to design the updating law of ILC; therefore, these methods are in the direct ILC category. To the best knowledge of the authors, this article is the first work on ILC-based MPC, or L-MPC.

To evaluate the proposed algorithm, it is applied to closed-loop control of an artificial pancreatic β-cell for Type 1 diabetes mellitus (T1DM). T1DM is a metabolic disease characterized by damaged β-cells, which are responsible for insulin secretion. In 2000, ~17.1 million persons worldwide have Type 1 diabetes mellitus,[8][9] and a clear rising trend in the incidence of the disease has been reported.[10] The hyperglycemia (high blood glucose concentration) resulting from insulin deficiency can cause many serious, long-term complications, such as heart disease, hypertension, retinopathy, nephropathy, and neuropathy. To reduce the glucose level, exogenous insulin delivery is required for subjects with T1DM. However, excessive insulin infusion can result in hypoglycemia (low blood glucose concentration), which will cause impaired brain functions or even death.[11] Hence, managing the insulin delivery to achieve normal glucose levels is a daily challenge.

MPC has been used previously for glycemia control.[12][13] Because of the clinical disturbances, e.g., meals, the glucose level controlled by MPC is not flat enough if the set-point is fixed to be the target. On the other hand, people generally consume meals at the similar time from day to day; hence the glucose-meal-insulin dynamics can be considered a continuous process with periodic disturbances. This is the main motivation for using L-MPC for the artificial pancreatic β-cell. The following simulation results will illustrate that the ILC-based set-point can substantially improve the control performance of MPC.

The rest of this article is organized as follows: A nonlinear physiological model describing the virtual subject and an auto-regressive exogenous (ARX) model for control design are introduced in "Virtual Subject and ARX Model." The controller is designed in "Learning-Type Model Predictive Control," where the MPC-based local controller and the ILC-based set-point are introduced separately. "Experiment Results" presents numbers of simulation results that demonstrate the excellence of the proposed method. Finally, some conclusions are provided in "Conclusions."

Virtual Subject and ARX Model

In previous studies,[14-16] an *in silico* model for T1DM was proposed. This *in silico* subject is comprised of three subsystems: the glucose subsystem, the insulin subsystem, and the meal subsystem. The glucose subsystem is described as a two-compartment model (glucose mass in plasma and rapidly equilibrating tissues; glucose mass in slowly equilibrating tissues); another two-compartment model (periphery degradation and liver degradation) is used to describe insulin kinetics, and the meal subsystem is also assumed to be two compartments (one for the liquid and another for the solid phase). On the basis of this model, a simulation environment was built by researchers from University of Virginia and University of Padova,[17] named the UVa/Padova diabetes simulator for short. The core of the simulation environment is a set of *in silico* subjects. In this work, 11 *in silico* subjects (adults 1-10 and adult average) from the simulator were used in a virtual subject platform built in MATLAB® (The MathWorks, Natick, MA).

An identification technique is required to develop a model of the virtual subject for controller design, because the aforementioned physiological model serves only as the virtual subject. In clinical practice, the available variables for model identification are insulin delivery rate, glucose concentration, and carbohydrate (CHO) count; however, the CHO count needs to be estimated by a human, so an accurate value is difficult to determine. Therefore, an ARX model will be used to approximate the relationship between the insulin and the glucose levels. For this study, the input, insulin delivery rate, is denoted as $u(t)$ and the output, glucose concentration, is denoted as $y(t)$, where t is the time step index. The sample time is set at 5 min, in accordance with the DexCom Seven® system.[18]

To develop the model between insulin and glucose levels, an open-loop experiment without meals (i.e., fasting condition) is conducted on the virtual subject for 24 h. The insulin delivery rate has a step change, so the step-response identification method can be used to identify the model between $u(t)$ and $y(t)$. For simplicity, an ARX model is used to approximate this relationship, as shown here.

$$A(z^{-1})y(t) = B(z^{-1})u(t - nd) + w(t) \quad (1)$$

where z^{-1} is the backward shift operator, nd is the time delay, and $w(t)$ denotes uncertainties or disturbances.

Learning-Type Model Predictive Control

Model predictive control

A short overview of the basic MPC algorithm is provided here; a more detailed overview of MPC can be found in textbooks, for example the book.[19] The key algorithmic components of MPC include: prediction model, cost function, and receding horizon optimization. On the basis of the ARX model in Eq. 1, the prediction model can be built. Given that the set-point for MPC is $y_r(t)$, the cost function is given as

$$\Omega \triangleq \sum_{j=1}^{N} \alpha_1 \left(y_r(t+j) - \hat{y}(t+j|t)\right)^2 + \sum_{i=0}^{M} \left[\alpha_2 \left(u(t+i|t)\right)^2 + \alpha_3 \left(\Delta u(t+i|t)\right)^2\right] \quad (2)$$

where the integers N and M ($N > M$) are referred to, respectively, as the prediction horizon and control horizon. $\hat{y}(t+j|t)$ denotes the prediction of $y(t+j)$ based on the known information at time t. $u(t+i|t)|_{i=0}^{M}$ denotes the possible control sequence in the control horizon, and Δu denotes variations of the control signal over time. Weights α_1, α_2, and α_3 adjust the relative importance of tracking error suppression, input penalty, and input variation penalty, respectively. Guidelines for choosing $\{N,M,\alpha_1,\alpha_2,\alpha_3\}$ can be found in the literature.[19] The following optimization problem is solved to obtain the updating law:

$$u(t+i|t)|_{i=0}^{M} = \underset{u(t+i|t)}{\arg\min}\, \Omega \quad (3)$$

In this work, the optimization problem (3) is solved using the MPC toolbox in MATLAB. After a feasible solution $u(t+i|t)|_{i=0}^{M}$ is obtained, only the first term $u(t|t)$ is implemented; at time $t + 1$, the optimization procedure will be repeated.

Learning-type set-point

Because of the repetitive nature of meal intake, glucose measurement, and insulin delivery over a 24-h period, the glucose-meal-insulin dynamics can be interpreted as a continuous process with periodic disturbances. Therefore, the tracking error from the previous day can be used to adjust the set-point in the current day. Because the period of the characteristic dynamics is 24 h and the sample time is 5 min, the period for time step t is $T = 288$. Hence, t and $t-T$

correspond to the same moment in two neighboring days, so the meal disturbances at these two points are the same or similar. It is reasonable to assume that

$$y_r(t) - y(t) \approx y_r(t-T) - y(t-T) \quad (4)$$

On the basis of this assumption and given the tracking error $e(t - T) = Y_r - y(t - T)$, one obtains

$$\begin{aligned} e(t) &= Y_r - y(t) = Y_r - y_r(t) + y_r(t) - y(t) \\ &\approx Y_r - y_r(t) + y_r(t-T) - y(t-T) \\ &= e(t-T) + y_r(t-T) - y_r(t) \end{aligned} \quad (5)$$

Letting $e(t) = 0$ in (5), the "optimal" choice for the set-point $y_r(t)$ is

$$y_r(t) = y_r(t-T) + e(t-T) \quad (6)$$

however, this aggressive scheme might lead to overshoot, which should be avoided; hence, a more reasonable and robust scheme is introduced for updating the set-point

$$y_r(t) = y_r(t-T) + Ke(t-T); \quad y_r(t) \equiv Y_r, \text{when } t \in [0, T) \quad (7)$$

This is a typical P-type ILC,[20][21] where $0 < K < 1$ is the learning gain.

In the literature,[22] a sufficient condition for asymptotical stability of a closed-loop system under indirect ILC was established. Under this condition, the tracking error $e(t)$ will converge to zero. Therefore, according to (7), $y_r(t)$ will be similar to $y_r(t - T)$, in other word, the ILC-based set-point will converge to a periodic profile. The range of the limit periodic profile could be great, which is a potential risk when there exist batch-wise variations; hence, some constraints on the set-point is introduced in (12).

In other words, within the L-MPC framework, MPC works as the local control; an ILC is used to update the set-point for MPC. For clarity, the block diagram of L-MPC is shown in Figure 2.

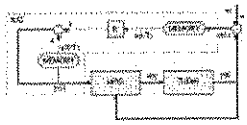

Figure 2. Block diagram of learning-type model predictive control.The solid arrow lines denote the real-time information; the dotted arrow lines denote the information in the previous cycle; components in the dashed frame comprise an iterative learning controller (ILC). [Color figure can be viewed in the online issue, which is available at www.interscience.wiley.com.]
[Normal View 16K | Magnified View 37K]

Experiment Results

Controller design

The following simulations are completed on the Adult Average subject from the UVa/Padova diabetes simulator. An open-loop simulation is performed to identify the model in Eq. 1. The insulin delivery rate is chosen as

$$u(t) = \begin{cases} 0.6\,\text{U/h}, & 0 \le t < 60 \\ 0.5\,\text{U/h}, & 60 \le t \le 144 \end{cases} \quad (8)$$

Then, the ARX model can be obtained as shown below

$$\begin{aligned} A(z^{-1}) &= 1 - 1.9860z^{-1} + 0.9864z^{-2}; \\ B(z^{-1}) &= -0.0030; \; nd = 1 \end{aligned} \quad (9)$$

Obviously, it is impossible to describe the virtual subject (comprised of three nonlinear sub-models introduced in "Virtual Subject and ARX Model") accurately by using this simplified model. Next, the control law will be designed, based on the simplified model in (9).

To compare the tracking performance in different cases numerically, the following criterion is introduced

(10)

$$\mathrm{ATE}(k) \triangleq \sum_{t=(k-1)T+1}^{kT} |y(t) - Y_r|/T$$

which is the average tracking error (ATE) for *k*th day. Obviously, a smaller ATE equates to a better tracking performance.

Because the glucose-insulin dynamics are relatively slow, the prediction horizon is chosen as 50; for tuning, the control horizon is chosen as 5. In the MPC module, three weights need to be designed: the tracking error weight α_1, the input penalty weight α_2, and the input variation penalty weight α_3. Three parameters can be combined to yield two degree of freedom: if α_3 is fixed to be unit, only α_1 and α_2 should be tuned. The ATE values of MPC and L-MPC are compared in Figure 3 under four groups of weights: $\{\alpha_1,\alpha_2,\alpha_3\}$ = {2.5,1,1}, {10,1,1}, {5,0.5,1}, or {5,2,1}, respectively. It is clear that MPC is robust to different weight settings and L-MPC can improve the closed-loop performance in all cases. On the basis of the simulation results, intermediate values are chosen in this study: $\alpha_1 = 5$, $\alpha_2 = 1$, and $\alpha_3 = 1$. To guarantee continuous insulin delivery, the following constraint is introduced:

$$u(t) \geq 0.24\ \mathrm{U/h} \qquad 11$$

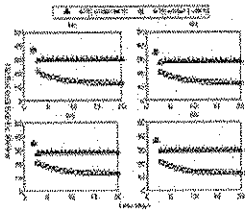

Figure 3. Comparison of average tracking error under different weights.Where △ denotes ATE for MPC and O denotes ATE for L-MPC: (a) {α1, α2, α3} = {2.5,1,1}; (b) {α1, α2, α3} = {10,1,1}; (c) {α1, α2, α3} = {5,0.5,1}; (d) {α1, α2, α3} = {5,2,1}. [Color figure can be viewed in the online issue, which is available at www.interscience.wiley.com.] [Normal View 34K | Magnified View 87K]

Other than the set-point, all parameters are the same for L-MPC and MPC.

Repetitive diets

In this section, it is assumed that the subject consumes three meals a day at {7:00, 13:00, and 18:00} with fixed amounts of carbohydrate, {60 g, 100 g, and 70 g}, respectively. In the first day, an optimized basal and bolus open-loop therapy is used as follows: the basal rate is subject-specific as defined in the UVa/Padova simulator, and meal-related boluses are calculated using subject-specific insulin-to-carbohydrate ratios and meal sizes. The feedback control is engaged on the second day. The target for output is chosen as Y_r = 110 mg/dl. In this work, hyperglycemia is defined as blood glucose concentration greater than 180 mg/dl.[23] While the definition of hypoglycemia has a wide range (60-70 mg/dl)[24] and is associated with or without clinical symptoms. For simplicity, we have selected 60 mg/dl as hypoglycemia threshold where any deviations below this level are termed significant hypoglycemia.[24][25] Accordingly, blood glucose concentrations between 60 mg/dl and 180 mg/dl are considered to be within the safe range for T1DM.

For ILC, only the learning gain needs to be designed. The ATE values for three different learning gains are compared in Figure 4. The ILC does not begin to adjust the set-point in the first day, so the ATE values in this day are the same and, hence, are omitted. Evidently, larger *K* values result in faster convergence rates in the cycle direction; however, larger *K* values will induce worse robustness to variations. In this article, an intermediate value of $K = 0.5$ is chosen to strive a compromise between these two effects.

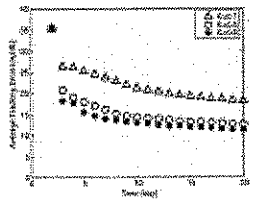

Figure 4. Comparison of average tracking error for three different learning gains.[Color figure can be viewed in the online issue, which is available at www.interscience.wiley.com.] [Normal View 21K | Magnified View 54K]

The control results under L-MPC for 20 days are given in Figure 5: Figure 5a shows the glucose levels for 20 days; Figure 5b shows the insulin delivery rates; for clarity, the glucose and insulin curves in the last day are enlarged in Figures 5c, d, respectively. For comparison, Figure 6 shows the control results under MPC for 20 days. From Figure 6a, one can see that the control performance becomes steady after the 3rd day. As shown in Figure 6c, the range of glucose concentrations under MPC is about 68-201 mg/dl. For the L-MPC case, as shown in Figure 5a, the control performance keeps improving from day to day, and the glucose level in the last day can remain in the range of about 68-145 mg/dl, as shown in Figure 5c, which is excellent for T1DM. Clearly, L-MPC can improve the control performance over MPC.

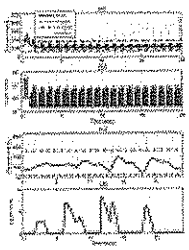

Figure 5. Control performance under L-MPC in 20 days.(a) Glucose level, safe range, and set-point; (b) insulin delivery rate, where logarithmic scale was used for the Y-axis; (c) last day's results; (d) last day's insulin. [Color figure can be viewed in the online issue, which is available at www.interscience.wiley.com.]
[Normal View 46K | Magnified View 149K]

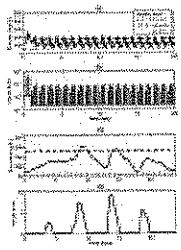

Figure 6. Control performance under MPC in 20 days.(a) Glucose concentration; (b) insulin delivery rate, where logarithmic scale was used for the Y-axis; (c) last day's glucose; (d) last day's insulin. [Color figure can be viewed in the online issue, which is available at www.interscience.wiley.com.]
[Normal View 43K | Magnified View 128K]

In most cases, it is difficult or even impossible to achieve exact tracking due to unmeasured disturbances, constraints, and other uncertainties. Therefore, the set-point will keep updating such that it has a large variation, as shown in Figure 5a. The excessive range of the set-point creates potential risks, especially in the presence of non-repetitive variations, such as meal amount and timing variations. To avoid the potential risks and improve L-MPC's robustness, some limitations are added to the ILC-based set-point:

$$y_r(t) = \max\{\delta_1 Y_r,\ \min[\delta_2 Y_r,\ y_r(t-T) + Ke(t-T)]\} \qquad 12$$

where $0 < \delta_1 < 1$ and $\delta_2 > 1$ are designed parameters. In fact, these limitations conduce a boundary layer for the set-point, and the thickness of the layer is $(\delta_2 - \delta_1)Y_r$. Therefore, a larger $\delta_2 - \delta_1$ will introduce more freedom for L-MPC but may result in worse robustness. In practice, δ_1 and δ_2 can be designed based on the acceptable range for the output. As an example, because the immediate danger from hypoglycemia (glucose concentrate lower than 60 mg/dl) is much greater than that from hyperglycemia (glucose concentration higher than 180 mg/dl), $\delta_1 = 0.7$ and $\delta_2 = 2$ were chosen in this work, so the range for the set-point is between 77 mg/dl (>60 mg/dl) and 220 mg/dl. The control results under constrained L-MPC are shown in Figure 7.

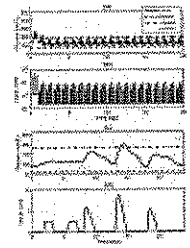

Figure 7. Control performance under constrained L-MPC in 20 days.(a) Glucose concentration; (b) insulin delivery rate, where logarithmic scale was used for the Y-axis; (c) last day's glucose; (d) last day's insulin. [Color figure can be viewed in the online issue, which is available at www.interscience.wiley.com.]
[Normal View 44K | Magnified View 135K]

As shown in Figures 5 and 7, L-MPC eventually gives bolus-like patterns to compensate for meals. In addition, nocturnal insulin delivery has been redesigned by the algorithm in the form of extended bolus to optimize fasting insulin requirements for a set-point of 110 mg/dl.

ATE values for MPC, L-MPC, and constrained L-MPC are compared in Figure 8. The ATE values under MPC remain constant from the 4th day, while the ATE values under L-MPC and constrained L-MPC continuous to decrease. The ATE values in the last day are 12.6, 21.4, and 28.6, respectively, under L-MPC, constrained L-MPC, and MPC. L-MPC exhibits better performance than constrained L-MPC, which may be explained by the difficulty of obtaining rapid insulin boluses without allowing large variations in the set-point. Both L-MPC and constrained L-MPC have superior performance over MPC. In subsequent sections, only constrained L-MPC is used; for convenience, the terminology "constrained" is omitted.

Figure 8. Comparison of average tracking error for MPC, L-MPC, and constrained L-MPC.[Color figure can be viewed in the online issue, which is available at www.interscience.wiley.com.]

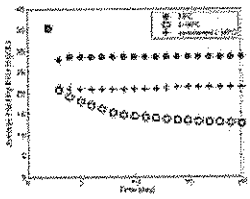

[Normal View 22K | Magnified View 55K]

Robustness to meal variations

In the previous sections, it is assumed that the sizes and timings of meals remain the same from day to day. For practical application, the proposed algorithm should be able to remain effective in the presence of significant variations. Hence, the robustness of L-MPC in the presence of variations in meal amounts and meal timings must be studied. The effects of each factor on the control performance are considered separately at first, then in combination. The nominal values for meal amounts and meal timings are still set at {60 g, 100 g, 70 g} and {8:00, 13:00, 18:00}.

To study the effects of variations in meal amounts, the meal times are fixed. A uniform distributed random variable is added independently to the nominal meal amount. The statistical results are given in Table 1. For variations as large as ±75%, the minimum size of lunch is 25 g and the maximum size is 175 g, which is quite a large difference; however, the control performance is still acceptable. The glucose and insulin curves over 20 days are given in Figures 9a, b, respectively. For clarity, the control results in the last day are shown in Figures 9c, d. The proposed scheme has excellent robustness in the presence of meal amount variations.

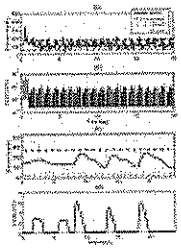

Figure 9. Control results of average subject with ±75% variation in meal amounts.(a) Glucose curve; (b) insulin curve, where logarithmic scale was used for the Y-axis; (c) last day's glucose; (d) last day's insulin. [Color figure can be viewed in the online issue, which is available at www.interscience.wiley.com.]
[Normal View 45K | Magnified View 139K]

Table 1. Robustness Statistic Results for L-MPC

	Mean ATE (mg/dl)	Percentage of Hyperglycemia	Percentage of Hypoglycemia	Percentage in Safe Range
Nominal	21.45	4.85%	0.00%	95.15%
±25%	21.60	4.05%	0.00%	95.95%
±50%	22.51	5.52%	0.51%	93.97%
±75%	24.62	7.05%	2.12%	90.84%
±20 min	22.05	4.89%	0.16%	94.95%
±40 min	23.04	4.69%	1.07%	94.24%
±60 min	24.32	4.51%	1.96%	93.53%
±50% and ±40 min	24.81	6.55%	1.65%	91.81%

For each case, 110 days' simulations were done, and the last 100 days' simulation results are analyzed in this table. Mean ATE is the average of the last 100 days' ATE.

Now, the meal amounts are fixed in nominal values so that the effects of meal time variations may be studied. As shown in Table 1, the robustness of L-MPC to meal time variations is impressive: performance indices in all cases are very close to those in nominal cases. If the variation range is ±60 min, the duration between two meals in some cases will be as short as 3 h or as long as 7 h. According to our experience, this is wide enough to describe real life uncertainties for most individuals. The control results with ±60 min variations are shown in Figure 10, which validates the superior robustness of L-MPC to account for meal timing variations.

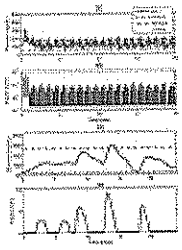

Figure 10. Control results of average subject with ±60 min variation in meal times.(a) Glucose curve; (b) insulin curve, where logarithmic scale was used for the Y-axis; (c) last day's glucose; (d) last day's insulin. [Color figure can be viewed in the online issue, which is available at www.interscience.wiley.com.]
[Normal View 44K | Magnified View 134K]

The previous results consider the robustness of L-MPC to meal amount and meal timing variations separately; however, these variations can appear together in real life. In the next phase, it is assumed that there are both meal size variations within ±50% and meal timing variations within ±40 min. The control performance indices are also included in Table 1. The control results for 20 days are shown in Figure 11. These results demonstrate that L-MPC has very good robustness to real-life variations in diet.

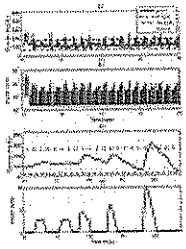

Figure 11. Control results of average subject with (±50%, ±40 min) meal variations.(a) Glucose curve; (b) insulin curve, where logarithmic scale was used for the Y-axis; (c) last day's glucose; (d) last day's insulin. [Color figure can be viewed in the online issue, which is available at www.interscience.wiley.com.]
[Normal View 45K | Magnified View 133K]

Robustness to subject variations

The preceding results were all conducted on the Adult Average subject. In clinic, biometric values such as weights, insulin resistances, and ages have wide distributions. A good therapy should be robust enough to treat a reasonable distribution in the population.

In this section, Adults 1-10 are tested under L-MPC. Except for the ARX models identified by using the step-response identification method, all other parameters for L-MPC are the same as those used for the Adult Average subject. All control results for the 10 subjects under L-MPC are shown in Figure 12.

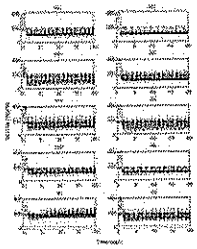

Figure 12. Control results of 10 subjects under L-MPC.Where a constant insulin delivery rate, 0.6 U/h, was used in the first day to challenge the proposed algorithm. Subfigures (a)-(j) correspond to Adults 1-10 respectively. The meals are repetitive and the same in all cases. [Color figure can be viewed in the online issue, which is available at www.interscience.wiley.com.]
[Normal View 50K | Magnified View 155K]

From Figure 12, it is seen that the control performance can be improved from day to day for most subjects, which is one of the advantages of L-MPC. After a few days, an absolute majority of glucose values have converged within the safe range with little variation in all 10 cases. This demonstrates that L-MPC has good robustness to subject variations. It should be noted that using fixed parameters for all subjects results in suboptimal control results for some cases (e.g., Adult 9), which can be easily fixed by adjusting controller parameters. To highlight the function of learning, Figure 13 compares the ATE values for 10 subjects under L-MPC and MPC. In all cases, the tracking performance under L-MPC is better than that under MPC, due to the function of ILC-based set-point. The values of ATE in the last day for two control algorithms are compared for the 10 cases, and L-MPC reduce ATE by 21.1% in average.

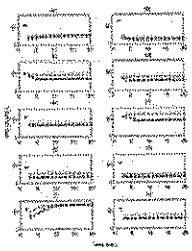

Figure 13. Comparison of tracking performance for 10 subjects under MPC and L-MPC, respectively. "+" denotes ATE for MPC; "*" denotes ATE for L-MPC. Subfigures (a)-(j) correspond to Adults 1-10 respectively. [Color figure can be viewed in the online issue, which is available at www.interscience.wiley.com.]
[Normal View 38K | Magnified View 113K]

Conclusions

This is the first work using ILC to adjust the set-point for MPC, a method termed L-MPC in this work. To validate this novel combination, the proposed method was implemented in the artificial pancreatic β-cell for T1DM. By exploiting the repetitive nature of the glucose-meal-insulin dynamics, the control performance under L-MPC can be improved from day to day. It has been shown that the proposed algorithm is robust to meal variations and subject variability. In addition, this algorithm does not rely on the subject's intervention, so, it will be suitable for pediatric populations and for those who do not wish to take control of their diabetes.

The design of ILC is independent of the local controller, so the proposed ILC can be transplanted to combinations with other methods, such as internal model control, PID control, and H_{∞} control. In addition, whereas only output regulation is considered in this article for simplicity, the proposed idea can be implemented for output tracking issue.

Notation

Indices

$A(z^{-1})$ auto-regressive function for ARX model, dimensionless

ATE average tracking error, mg/dl

$B(z^{-1})$ exogenous function for ARX model, dimensionless

nd time delay, dimensionless

T period for the continuous process, dimensionless

t time-step index, multiplier of the sample time (5 min), dimensionless

z^{-1} backward shift operator, dimensionless

Ω cost function for MPC, dimensionless

Parameters

K learning gain, dimensionless

M control horizon, dimensionless

N prediction horizon, dimensionless

α_1 weight for tracking error suppression in the cost function, dimensionless

α_2 weight for input penalty in the cost function, dimensionless

α_3 weight for input variation penalty in the cost function, dimensionless

δ_1 a design parameter for the lower boundary of the set-point, dimensionless

δ_2 a design parameter for the upper boundary of the set-point, dimensionless

Variables

$e(\cdot)$ output tracking error, mg/dl

$u(\cdot)$ input, insulin delivery rate, U/h

$w(t)$ uncertainties or disturbances, dimensionless

Y_r target for the output, mg/dl

$y(\cdot)$ output, glucose concentration, mg/dl

$y_r(\cdot)$ set-point for MPC, mg/dl

$\hat{y}(\cdot)$ the prediction of the output $y(\cdot)$, mg/dl

Acknowledgements

This work is supported by Grant # 22-2007-1801 from the Juvenile Diabetes Research Foundation (JDRF) and the Otis Williams Fund at the Santa Barbara Foundation.

REFERENCES

1 Isidori A. *Nonlinear Control Systems*, 3rd ed. London: Springer-Verlag London Limited, 1995.

2 Wang YQ, Gao FR, Doyle FJ III. Survey on iterative learning control, repetitive control, and run-to-run control. *J Process Control*. In press. Links

3 Tan KK, Zhao S, Xu J-X. Online automatic tuning of a proportional integral derivative controller based on an iterative learning control approach. *IET Control Theory Appl.* 2007; **1**: 90-96. Links

4 Wu JH, Ding H. Reference adjustment for a high-acceleration and high-precision platform via A-type of iterative learning control. *Proc IMechE Part I: J Syst Control Eng.* 2007; **221**: 781-789. Links

5 Lee KS, Chin IS, Lee HJ. Model predictive control technique combined with iterative learning for batch processes. *AIChE J.* 1999; **45**: 2175-2187. Links

6 Shi J, Gao FR, Wu TJ. Single-cycle and multi-cycle generalized 2D model predictive iterative learning control (2D-GPILC) schemes for batch processes. *J Process Control.* 2007; **17**: 715-727. Links

7 Wang Y, Dassau E, Doyle FJ III. Closed-loop control of artificial pancreatic β-cell in type 1 diabetes mellitus using model predictive iterative learning control. *IEEE Trans Biomed Eng.* http://ieeexplore.ieee.org/stamp/stamp.jsp?tp=&arnumber=5072274&isnumber=4359967. Links

8 Eiselein L, Schewartz HJ, Rutledge JC. The challenge of type 1 diabetes mellitus. *ILAR J.* 2004; **45**: 231-236. Links

9 Wild S, Roglic G, Green A, Sicree R, King H. Global prevalence of diabetes: estimates for the year 2000 and projections for 2030. *Diab Care.* 2004; **27**: 1047-1053. Links

10 Gale EAM. Spring harvest? Reflections on the rise of type 1 diabetes. *Diabetologia.* 2005; **48**: 2445-2450. Links

11 Teixeira RE, Malin S. The next generation of artificial pancreas control algorithms. *J Diabetes Sci Technol.* 2008; **2**: 105-112. Links

12 Parker RS, Doyle FJ III, Peppas NA. The intravenous route to blood glucose control. *IEEE Eng Med Biol Mag.* 2001; 65-73. Links

13 Hovorka R, Canonico V, Chassin LJ, Haueter U, Massi-Benedetti M, Federici MO, Pieber TR, Schaller HC, Schaupp L, Vering T, Wilinska ME. Nonlinear model predictive control of glucose concentration in subjects with type 1 diabetes. *Physiol Meas.* 2004; **25**: 905-920. Links

14 Dalla Man C, Camilleri M, Cobelli C. A system model of oral glucose absorption: validation on gold standard data. *IEEE Trans Biomed Eng.* 2006; **53**: 2472-2478. Links

15 Dalla Man C, Rizza RA, Cobelli C. Meal simulation model of the glucose-insulin system. *IEEE Trans Biomed Eng.* 2007; **54**: 1740-1749. Links

16 Dalla Man C, Raimondo DM, Rizza RA, Cobelli C. GIM, simulation software of meal glucose-insulin model. *J Diabetes Sci Technol.* 2007; **1**: 323-330. Links

17 Kovatchev BP, Breton MD, Dalla Man C, Cobelli C. *In silico* preclinical trials: a proof of concept in closed-loop control of type 1 diabetes. *J. Diabetes Sci Technol.* 2009; **3**: 44-55. Links

18 Kovatchev B, Anderson S, Heinemann L, Clarke W. Comparison of the numerical and clinical accuracy of four continuous glucose monitors. *Diab Care.* 2008; **31**: 1160-1164. Links

19 Camacho EF, Bordons C. *Model Predictive Control in the Process Industry. Advances in Industrial Control.* London: Springer-Verlag London Limited, 1995.

20 Ye YQ, Wang DW. Learning more frequency components using P-type ILC with negative learning gain. *IEEE Trans Ind Electron.* 2006; **53**: 712-716. Links

21 Chi R, Hou Z, Xu J. Adaptive ILC for a class of discrete-time systems with iteration-varying trajectory and random initial condition. *Automatica.* 2008; **44**: 2207-2213. Links

22 Wang Y, Doyle FJ III. Stability analysis for set-point-related indirect iterative learning control. Submitted to 48th IEEE Conference on Decision and Control, 2009.

23 The diabetes control and complications trial research group (DCCT). The effect of intensive treatment of diabetes on the development and progression of long-term complications in insulin-dependent diabetes mellitus. *N Engl J Med.* 1993; **329**: 977-986. Links

24 Frier BM. Defining hypoglycaemia: what level has clinical relevance? *Diabetologia.* 2009; **52**: 31-34. Links

25 Dua P, Doyle FJ III, Pistikopoulos EN. Model-based blood glucose control for type 1 diabetes via parametric programming. *IEEE Trans Biomed Eng.* 2006; **53**: 1478-1491. Links

Detection of a Meal Using Continuous Glucose Monitoring

Implications for an artificial β-cell

EYAL DASSAU, PHD[1]
B. WAYNE BEQUETTE, PHD[2]
BRUCE A. BUCKINGHAM, MD[3]
FRANCIS J. DOYLE, III, PHD[1]

OBJECTIVE — The purpose of this study was to introduce a novel meal detection algorithm (MDA) to be used as part of an artificial β-cell that uses a continuous glucose monitor (CGM).

RESEARCH DESIGN AND METHODS — We developed our MDA on a dataset of 26 meal events using records from 19 children aged 1–6 years who used the MiniMed CGMS Gold. We then applied this algorithm to CGM records from a DirecNet pilot study of the FreeStyle Navigator continuous glucose sensor. During a research center admission, breakfast insulin was withheld for 1 h, and discrete glucose levels were obtained every 10 min after the meal.

RESULTS — Based on the Navigator readings, the MDA detected a meal at a mean time of 30 min from the onset of eating, at which time the mean serum glucose was 21 mg/dl above baseline (range 2–36 mg/dl), and >90% of meals were detected before the glucose had risen 40 mg/dl from baseline.

CONCLUSIONS — The MDA will enable automated insulin dosing in response to meals, facilitating the development of an artificial pancreas.

Diabetes Care 31:295–300, 2008

The development of an artificial β-cell is a challenging task that has drawn together different disciplines within engineering, science, and medicine for the past 30 years (1). In the most likely scenario, the subject is connected to both a continuous subcutaneous insulin infusion system and a continuous glucose monitor (CGM). The loop is "closed" inside a computer/personal data manager by software that regulates the glucose level by changing the insulin infusion rate of the pump. The success of such an artificial β-cell depends on the following: 1) predictive mathematical models of patients that can mimic glucose absorption secretion and insulin action (e.g., the pharmacokinetic/pharmacodynamic models in refs. 2 and 3); 2) reliable and accurate sensors that transmit real-time glucose measurements; 3) automated insulin pumps that can be controlled by software; and 4) a controller (algorithm) that can regulate glucose by changing the infusion rate based on sensor glucose measurements. A variety of controllers that are capable of regulating glucose can be found in the literature. Several are based on mathematical models and designed as proportional integral derivative or model predictive control (4–7); others are based on fuzzy logic (8). However, as was noted by Hovorka et al. (9), a number of challenges remain to be solved before the artificial β-cell is realized: one of the critical challenges is the regulation of glucose levels after a meal (10). The meal challenge can be met, in principle, by three different approaches. The first one is the feed-forward control approach in which the user of the artificial β-cell will inform the controller that a meal is occurring (or is about to occur) by clicking a button, thus initiating an insulin bolus. The second way is to rely strictly on feedback control, whereby the algorithm will respond only after a sufficiently large rise in glucose has occurred. This particular strategy has proven difficult in practice owing to the tradeoff between the need to respond quickly due to the delay in insulin absorption and the need to have a conservative scheme that does not deliver an overdose of insulin. The third approach is discrete meal detection; this will trigger an insulin bolus as part of an algorithm using continuous feedback from a CGM. One can envision that the first and third schemes could be combined, such that the discrete meal detection algorithm is a failsafe mode for a patient-initiated feed-forward scheme. This article details a reliable meal detection suite of solutions that was validated with historical CGM and can be implemented as part of an artificial β-cell controller.

RESEARCH DESIGN AND METHODS

— Meal-related glucose excursions were initially assessed using the data from 26 meal events when subjects were wearing a MiniMed Gold CGM (Medtronic Diabetes, Northridge, CA) and had marked the onset of a meal. These records were obtained from 19 children aged 1–7 years (mean age 5 years) who were participating in an outpatient study (11). The data presented here were taken from a DirecNet pilot study (a complete list of the participating centers and investigators can be found in the APPENDIX) of the FreeStyle Navigator real-time continuous subcutaneous glucose sensor (Abbott Diabetes Care, Alameda, CA) (12), which is currently an investigational device. This study of 30 children with type 1 diabetes treated with insulin infusion pump therapy included a clinical research center (CRC) admission.

From the [1]Department of Chemical Engineering, University of California Santa Barbara, Santa Barbara, California; the [2]Department of Chemical and Biological Engineering, Rensselaer Polytechnic Institute, Troy, New York; and the [3]Stanford Medical Center, Stanford, California.

Address correspondence and reprint requests to Francis J. Doyle III, Department of Chemical Engineering, University of California Santa Barbara, Santa Barbara, CA 93106-5080. E-mail: frank.doyle@icb.ucsb.edu.

Received for publication 6 July 2007 and accepted in revised form 21 October 2007.

Published ahead of print at http://care.diabetesjournals.org on 31 October 2007. DOI: 10.2337/dc07-1293.

B.W.B. serves on the Scientific Advisory Board of Ultradian Diagnostics. B.A.B. has received honoraria as a speaker for Abbott Diabetes Care.

Abbreviations: CGM, continuous glucose monitor; CRC, clinical research center; ROC, rate of change.

All subjects aged >8 signed an assent, and all parents signed a consent approved by the institutional review board at each participating DirecNet center. Twenty-one of the subjects had their breakfast dose of insulin withheld for 1 h to induce a rapid increase in blood glucose levels. Some children did not undergo this test because of their weight and the amount of previous blood sampling. For those participating in the meal challenge, blood samples were obtained every 10 min for 1 h after completion of breakfast. All subjects had been admitted to the CRC the previous day, and all were wearing a FreeStyle Navigator continuous glucose sensor that was recording interstitial blood glucose levels every minute. The average age of the subjects was 11 ± 4 years (range 4–17 years), and 40% were girls. Mean duration of diabetes was 6 ± 3 years. Mean A1C was 7.1 ± 0.6%.

Rate of change calculation

The glucose rate of change (ROC) is estimated by two different methods; both are based on real-time glucose measurements sampled at 1-min intervals. The first approach is a calculation of glucose ROC using a three-point (current and two previous samples) backward difference (13):

$$\frac{dG_i}{dt} = \frac{3G_i - 4G_{i-1} + G_{i-2}}{2\Delta t} \quad (1)$$

where G is the glucose measurement, t is time, Δt is the time difference between two sample intervals, and the subscripts i, $i-1$, and $i-2$ are the current and two previous samples, respectively.

The second approach is based on optimal estimation theory, using a Kalman filter (14,15), an established method that has been used as part of different algorithms in the context of glucose management such as the following: hypoglycemic/hyperglycemic prediction (16,17), improved glucose monitoring (18,19), and feedback control (7). This method assumes that the glucose sensor signal varies primarily through two contributions: *1*) real changes to the underlying glucose value (g_k) and 2) measurement noise (v_k). Hence, the glucose can be expressed in terms of its ROC (d_k):

$$g_{k+1} = g_k + d_k \quad (2)$$

such that the value at time $k + 1$ is the value at the previous time-step k plus the ROC. Similarly, the ROC can be expressed in terms of the rate in the previous time step plus the acceleration or the ROC of the ROC (f_k):

$$d_{k+1} = d_k + f_k \quad (3)$$

where the acceleration term is a stochastic signal that is changed by a random amount that can be interpreted as process noise (w_k):

$$f_{k+1} = f_k + w_k \quad (4)$$

where w_k has a mean value of 0 and a covariance of Q. The glucose measurement is corrupted by random measurement noise with zero mean and covariance R:

$$G_k = g_k + v_k \quad (5)$$

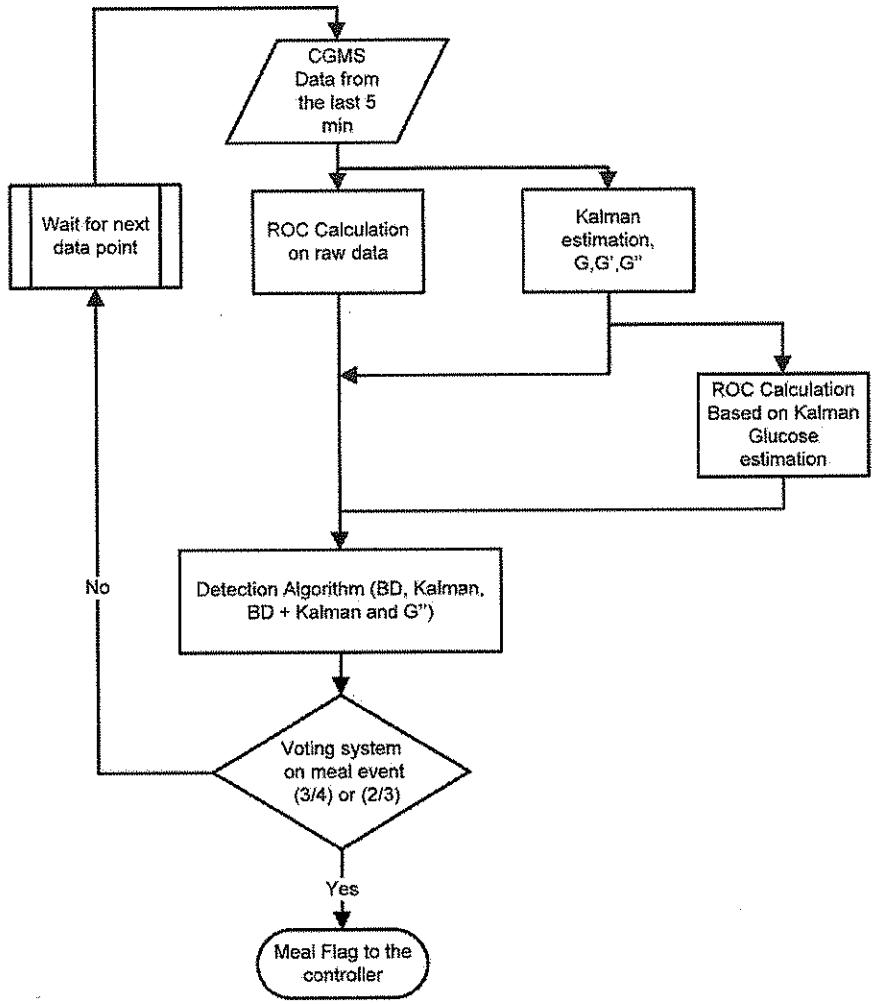

Figure 1— *Algorithm for implementing a safe meal detection that will minimize false-positive detection (invoking an unnecessary insulin bolus). The different detection methods are backward difference (BD), Kalman filter estimation (Kalman), combination of BD and Kalman (BD+Kalman), and second derivative of glucose (G"). The voting algorithm consists of either a two-out-of-three (BD, BD+Kalman, and G") or three-out-of-four (BD, Kalman, BD+Kalman, and G") scheme, respectively.*

Equations 2–5 can be written in matrix-vector form as

$$\begin{bmatrix} g \\ d \\ f \end{bmatrix}_{k+1} = \begin{bmatrix} 1 & 1 & 0 \\ 0 & 1 & 1 \\ 0 & 0 & 1 \end{bmatrix} \begin{bmatrix} g \\ d \\ f \end{bmatrix}_k + \begin{bmatrix} 0 \\ 0 \\ 1 \end{bmatrix} w_k \quad (6)$$

$$G_k = [1\ 0\ 0] \begin{bmatrix} g \\ d \\ f \end{bmatrix}_k + v_k \quad (7)$$

Equations 6 and 7 are commonly called discrete state space models, and the following notation is commonly used in the systems and control literature:

$$x_{k+1} = \Phi x_k + \Gamma^w w_k$$
$$y_k = C x_k + v_k \quad (8)$$

Table 1—*Results summary showing the meal times with the glucose value at the time of the meal with the four detections methods, detection time, and glucose level in deviation form from the onset of the meal value*

	Meal		BD		Kalman		BD + Kalman		G″	
Subject	Time	G (mg/dl)	ΔT (min)*	ΔG (mg/dl)†	ΔT (min)*	ΔG (mg/dl)†	ΔT (min)*	ΔG (mg/dl)†	ΔT (min)*	ΔG (mg/dl)†
01	7:28	134	27‡§	36	23	26	20	18	11	3
02	8:02	63	35‡	9	42§	35	21	9	38	19
03	8:04	218	30‡§	30	34	47	30	30	30	30
04	8:41	97	22‡	8	27	25	23§	11	20	3
06	8:31	263	27‡	2	39	24	37§	18	27	2
07	8:47	173	34	10	43	30	38‡§	18	38	18
08	8:17	88	36	4	50	27	49	24	37‡	5
09	7:33	106	10‡	5	19	22	12§	12	9	3
10	7:52	223	23	−4	32	39	28‡§	9	28	9
11	8:05	203	32	7	38	29	34§	12	33‡	10
12	7:34	105	40	5	47	28	42§	10	41‡	7
13	8:03	86	38‡	23	41	31	39§	25	34	16
14	8:14	85	33‡	27	34§	29	30	15	52	84
16	7:32	182	24‡	22	27	32	25§	26	19	11
17	8:07	146	18	8	35§	34	32	28	30‡	22
18	8:10	98	41	11	47	26	42§	13	41‡	11
20	9:02	175	17	9	24	35	20‡§	18	20	18
Average			29	13	35	30‖	31	18	30	16

*Detection time from the onset of the meal. †Difference between the glucose (G) level on detection minus the glucose level at onset of the meal. ‡Trigger of meal flag by the voting scheme algorithm of three-out-of-four methods, mean detection time of 32 min from the onset of eating, at which time the mean serum glucose was 21 ± 9 mg/dl above baseline. §Trigger of meal flag from the voting scheme algorithm of two-out-of-three (backward difference [BD], BD + Kalman filter estimation [Kalman], and G″) mean detection time of 30 min from the onset of eating, at which time the mean serum glucose was 15 ± 10 mg/dl above baseline. ‖The mean blood glucose using the Kalman algorithm was significantly higher compared with that using the other methods ($P < 0.001$).

where x is a vector of states and y is the measured output. In this application, the matrices and vectors have the following values:

$$\Phi = \begin{bmatrix} 1 & 1 & 0 \\ 0 & 1 & 1 \\ 0 & 0 & 1 \end{bmatrix}, \Gamma^w = \begin{bmatrix} 0 \\ 0 \\ 1 \end{bmatrix},$$

$$C = [1\ 0\ 0], x = \begin{bmatrix} g \\ d \\ f \end{bmatrix}, y = G \quad (9)$$

Because both the measurement and process noise are considered stochastic processes, their unknown covariances can be used as the tuning parameters. Hence, the tuning parameter used is related to the ratio of the expected process to sensor noise variance ($Q/R = 5 \times 10^{-6}$). The states are estimated using a predictor corrector equation of the form

$$\hat{x}_{k|k-1} = \Phi \hat{x}_{k-1|k-1} \quad (10)$$

$$\hat{x}_{k|k} = \hat{x}_{k|k-1} + L_k(y_k - C\hat{x}_{k|k-1}) \quad (11)$$

where $\hat{x}$ is the estimation of the states; the subscript $k|k-1$ indicates the estimation at time step k using the previous value; the process model is transformed using the standard notation (Φ, Γ, and C); and L is the Kalman gain. More details on the use of Kalman estimation in general and in the context of diabetes can be found in refs. 14–16.

The best estimate, at the current sample time, of the states (glucose, ROC of glucose, and ROC of the ROC of glucose) is

$$\begin{bmatrix} \hat{g} \\ \hat{d} \\ \hat{f} \end{bmatrix}_{k|k} = \hat{x}_{k|k} \quad (12)$$

In the discussion that follows, we will simply refer to these estimated states as G, G′, and G″; that is, at any sample time

$$\begin{bmatrix} G \\ G' \\ G'' \end{bmatrix} = \begin{bmatrix} \hat{g} \\ \hat{d} \\ \hat{f} \end{bmatrix}_{k|k} \quad (13)$$

Detection algorithm

The proposed algorithm for meal detection is divided into five stages as illustrated in the flowchart in Fig. 1 and detailed below (20):

1. The first stage is data acquisition, in which the last 5-min reading from the CGM is conveyed to the algorithm. These data are processed in parallel by a ROC component and a Kalman filter estimation algorithm.
2. In the second stage, the ROC estimation can be broken down into *1*) backward difference ROC calculation based on the raw data, *2*) backward difference estimation based on the glucose estimation from the Kalman filter (backward difference and Kalman), *3*) Kalman filter estimation of glucose (G) and the ROC (G′) (Kalman), and *4*) the Kalman estimate of the ROC of the ROC (G″). Thus, four separate inferences of the actual ROC are generated.
3. The estimated ROC is compared with a threshold value that corresponds to a meal-related rise in glucose and is screened using multiple heuristics to minimize false-positive detections. We have identified four design variables that can be tuned according to individual subjects: *1*) a glucose ROC threshold (1.8–3 mg/dl-min); *2*) a maximum glucose ROC (2–5 mg/dl-min); *3*) a glucose threshold (150–220 mg/dl); and *4*) an acceleration threshold (0.4–0.8 mg/dl per min^2). A sec-

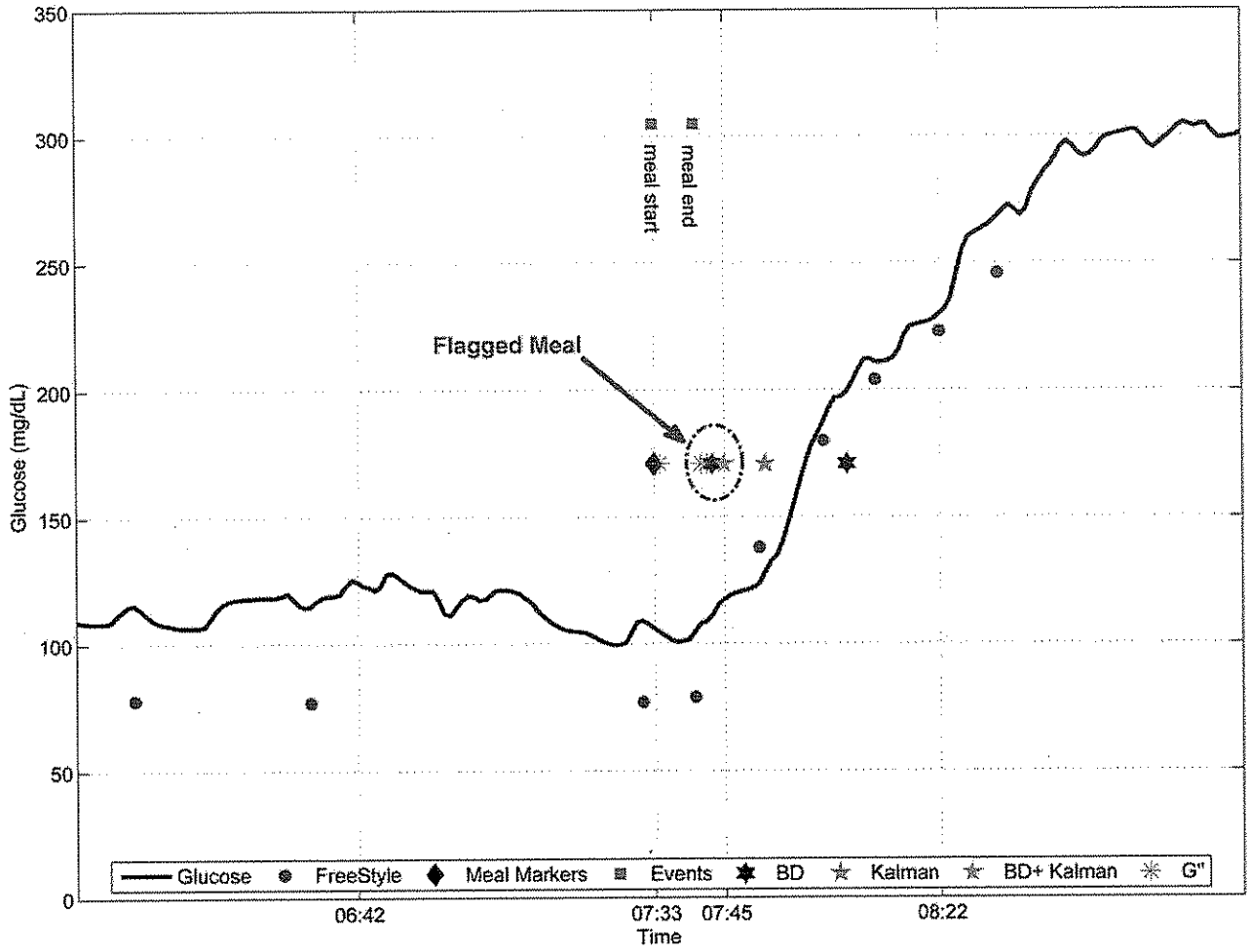

Figure 2— *A zoomed view of a sample of one data record of the challenged meal of a subject with meal detection using the four different methods (backward difference [BD], Kalman filter estimation [Kalman], combination of BD and Kalman [BD+Kalman], and second derivative of glucose [G"]).* ——, *real-time measurements that have been collected using CGMS;* ●, *freestyle finger stick data;* ■ *text, annotation of events including meal (start and/or stop) and snacks;* ♦, *meals were detected anywhere from 9 to 19 min from the onset, and the glucose level had increased by 3–22 mg/dl (20).*

ondary screening condition to minimize noise artifacts is the requirement that the glucose values will increase monotonically. As a safety interlock measure, a meal declaration will not be issued if such a declaration is issued 15–20 min earlier, and a night safety condition prevents any meal announcement during the night. This condition can be adjusted for the lifestyle of an individual patient. These safety layers can minimize false detections and lead to a more reliable automated system.

4. A voting algorithm is implemented to minimize the risk of an unnecessary insulin bolus. A meal flag will be sent only if two of three methods or three of four methods consistently detect a meal in the same 5-min time window.
5. Finally, the controller will receive a meal flag and/or the algorithm will reset for the next data point.

Statistics

Kruskal-Wallis one-way ANOVA on ranks was used to assess significance of the mean time from onset of the meal and the mean increase in glucose values from baseline when a meal was recognized by the four proposed algorithms (SigmaStat, SYSTAT, San Jose, CA).

RESULTS — The results from the 17 subjects admitted to the CRC as part of the DirecNet study (21) are summarized in Table 1. Subjects consumed an average of 56 g of carbohydrate for breakfast (range 22–105 g). The table details, for each meal detection method, the time it took to detect the meal (ΔT) and how much the glucose had increased from baseline when the meal was detected (ΔG). An example of meal detection is provided in Fig. 2. In this example, the four different methods succeeded in detecting the breakfast meal within <20 min of the onset of that meal, and there was a <22 mg/dl increase of the glucose from the preprandial value. In this figure a false-positive meal detection is seen, where G'' detected a meal before breakfast. The voting scheme, however, would have prevented this from being a false-positive event. In Table 1 the meal detection time for each of the voting schemes (three-out-of-four and two-out-of-three methods) is denoted for each of the 17 breakfast meals. Using a voting scheme of three-out-of-four, the overall mean detection time from all datasets was 32 min with a mean increase in the serum glucose of 21 ± 9 mg/dl from the onset of eating.

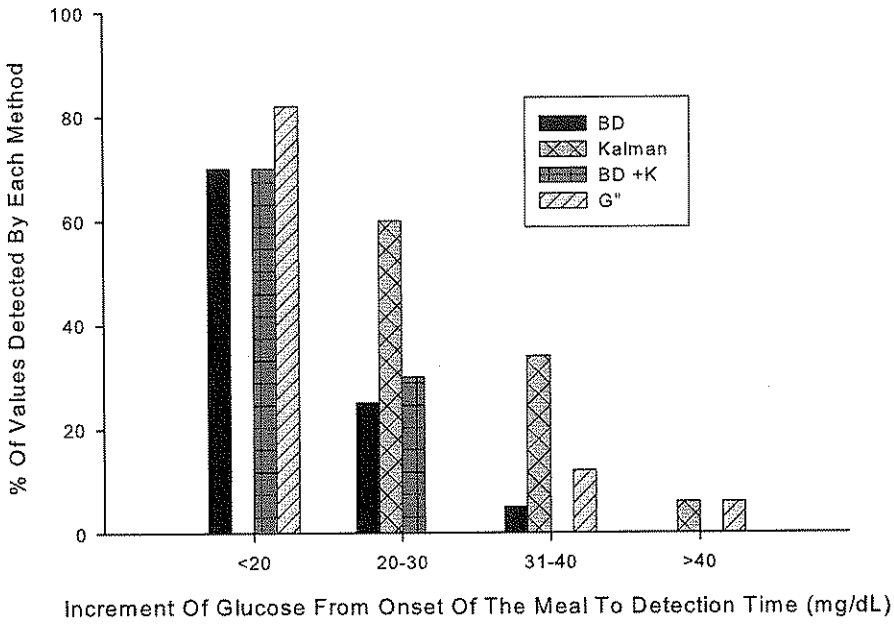

Figure 3— *Increment of glucose values from onset of the challenged meal until detection of the meal for the four different detection methods: backward difference (BD), Kalman filter estimation (Kalman), combination of BD and Kalman (BD+Kalman), and second derivative of glucose (G″).*

Using a voting scheme of two-out-of-three, the mean detection time was 30 min with a mean increase in the serum glucose of 15 ± 10 mg/dl from the onset of eating.

A summary of the results showing how well the "challenge" breakfast meal was detected in all 17 cases by the four different methods is presented in Table 1 and Fig. 3. The average detection time from the onset of the challenge meal was 29, 35, 31, and 30 min, respectively (Table 1), for the backward difference, Kalman, backward difference and Kalman, and *G″* algorithms, and the average detection time from the end of the meal was 11, 18, 13, and 12 min, respectively. The glucose only increased by a mean of 2 mg/dl from the onset of the meal to the completion of the meal, despite a mean of 17 min to complete a meal. One can infer from Fig. 3 that the Kalman estimation is more conservative than the other methods. This is a result of how the Kalman filter was tuned and, in our opinion, is beneficial in improving the robustness of the voting scheme and providing an additional layer of safety. A second critical factor is the increase in glucose by the time of meal detection. This information is presented in Fig. 3, which shows that 100, 94, 100, and 94% of meals were detected before a 40 mg/dl increase in the glucose using the backward difference, Kalman, backward difference and Kalman, and *G′* methods, respectively, and 94, 59, 100, and 94% of meals were detected before a 30 mg/dl increase in the glucose using the respective methods.

CONCLUSIONS— Meal detection is a critical and enabling component of a control algorithm for an artificial β-cell. Independent of whether one uses a proportional integral derivative, model predictive control, or another control algorithm, the ability to have an automated meal announcement that does not require patient input is an important factor. In reviewing the literature, we were unable to find another article in the medical or engineering literature that specifically addressed the issue of meal detection by using a continuous glucose sensor. We therefore evaluated meal detection algorithms using a FreeStyle Navigator that measures interstitial glucose. In addition, the insulin bolus for breakfast was delayed by 1 hour, allowing us to evaluate the ROC of glucose values following a meal without the confounding effects of an insulin bolus at the time of the meal. The content of the breakfast meals was decided by the study subject, and these meals varied significantly in their composition and grams of carbohydrate, as would occur in their home environment. These conditions therefore mimic the expected conditions for recognizing a meal in a fully closed-loop artificial β-cell.

A critical element of a meal detection algorithm is minimization of the time between the actual meal and the detection flag. This depends on a variety of factors including the meal composition, the time it took to consume the meal, insulin on board, and the amount of noise in the data. Using our algorithm that employed a voting scheme of two-out-of-three methods to detect a meal, the mean detection time from the onset of the meal was 30 min and the mean increase in the serum glucose was only 15 mg/dl. It is our impression that this algorithm combined with a rapid-acting insulin will provide the means to prevent significant postprandial hyper- and hypoglycemia in a closed-loop system, but this theory remains to be tested.

Acknowledgments— This work was supported by the Juvenile Diabetes Research Foundation through the artificial pancreas project (grant 22-2006-1108) and by the National Institutes of Health (grant R21-DK69833).

APPENDIX

The DirecNet Study Group clinical centers (listed in alphabetical order with clinical center name, city, and state. Personnel are listed as principal investigator [PI], coinvestigator [I], and coordinators [C]). *1*) Barbara Davis Center for Childhood Diabetes, University of Colorado, Denver, CO: Peter Chase (PI), Rosanna Fiallo-Scharer (I), Laurel Messer (C), and Barbara Tallant (C); 2) Department of Pediatrics, University of Iowa Carver College of Medicine, Iowa City, IA: Eva Tsalikian (PI), Michael J. Tansey (I), Linda F. Larson (C), Julie Coffey (C), and Joanne Cabbage (C); 3) Nemours Children's Clinic, Jacksonville, FL: Tim Wysocki (PI), Nelly Mauras (I), Larry A. Fox (I), Keisha Bird (C), and Kim Englert (C); 4) Division of Pediatric Endocrinology and Diabetes, Stanford University, Stanford, CA: Bruce A. Buckingham (PI), Darrel M. Wilson (I), Jennifer M. Block (C), Paula Clinton (C), and Kimberly Caswell; 5) Department of Pediatrics, Yale University School of Medicine, New Haven, CT: Stuart A. Weinzimer (PI), William V. Tamborlane (I), Elizabeth A. Doyle (C), Heather Mokotoff (C), and Amy Steffen (C). *Coordinating center*: Jaeb Center for Health Research, Tampa, FL: Roy W. Beck, Katrina J. Ruedy, Craig Kollman, Dongyuan Xing, Andrea Kalajian, and Cynthia R. Stockdale. *University of Minne-*

sota Central Laboratory: Michael W. Steffes, Jean M. Bucksa, Maren L. Nowicki, Carol A. Van Hale, and Vicky Makky. *National Institutes of Health:* Gilman D. Grave, Barbara Linder, and Karen K. Winer. *Data and Safety Monitoring Board:* Dorothy M. Becker, Christopher Cox, Christopher M. Ryan, Neil H. White, and Perrin C. White.

References

1. Hovorka R: Continuous glucose monitoring and closed-loop systems. *Diabet Med* 23:1–12, 2006
2. Dalla Man C, Camilleri M, Cobelli C: A system model of oral glucose absorption: validation on gold standard data. *IEEE Trans Biomed Eng* 53:2472–2478, 2006
3. Man CD, Toffolo G, Basu R, Rizza RA, Cobelli C: A model of glucose production during a meal. In *Conference Proceedings: Annual International Conference of the IEEE Engineering in Medicine and Biology Society.* Piscataway, NJ, IEEE Engineering in Medicine and Biology Society, 2006, p. 4
4. Marchetti G, Barolo M, Jovanovič L, Zisser H, Seborg DE: An improved PID switching control strategy for type 1 diabetes. In *Conference Proceedings: Annual International Conference of the IEEE Engineering in Medicine and Biology Society.* Piscataway, NJ, IEEE Engineering in Medicine and Biology Society, 2006, p. 4
5. Palerm CC, Zisser H, Bevier WC, Jovanovič L, Doyle FJ III: Prandial insulin dosing using run-to-run control: application of clinical data and medical expertise to define a suitable performance metric. *Diabetes Care* 30:1131–1136, 2007
6. Steil GM, Rebrin K, Darwin C, Hariri F, Saad MF: Feasibility of automating insulin delivery for the treatment of type 1 diabetes. *Diabetes* 55:3344–3350, 2006
7. Parker RS, Doyle FJ III, Peppas NA: A model-based algorithm for blood glucose control in type I diabetic patients. *IEEE Trans Biomed Eng* 46:148–157, 1999
8. Grant P: A new approach to diabetic control: fuzzy logic and insulin pump technology. *Med Eng Phys* 29:824–827, 2007
9. Hovorka R, Wilinska ME, Chassin LJ, Dunger DB: Roadmap to the artificial pancreas. *Diabetes Res Clin Pract* 74:S178–S182, 2006
10. Bequette BW: A critical assessment of algorithms and challenges in the development of a closed-loop artificial pancreas. *Diabetes Technol Ther* 7:28–47, 2005
11. Gandrud LM, Xing D, Kollman C, Block JM, Kunselman B, Wilson DM, Buckingham BA: The Medtronic MiniMed Gold continuous glucose monitoring system: an effective means to discover hypo- and hyperglycemia in children under 7 years of age. *Diabetes Technol Ther* 9:307–316, 2007
12. Wilson DM, Beck RW, Tamborlane WV, Dontchev MJ, Kollman C, Chase P, Fox LA, Ruedy KJ, Tsalikian E, Weinzimer SA, the DirecNet Study Group: The accuracy of the FreeStyle Navigator continuous glucose monitoring system in children with type 1 diabetes. *Diabetes Care* 30: 59–64, 2007
13. Riggs. JB: *An Introduction to Numerical Methods for Chemical Engineers.* Lubbock, Texas Tech University Press, 1994
14. Stengel RF: *Optimal Control and Estimation.* New York, Dover Publications, 1994
15. Bequette BW: Optimal estimation applications to continuous glucose monitoring. In *Proceedings of the American Control Conference.* Vol. 1. Boston, MA, IEEE, 2004, p. 958–962
16. Palerm CC, Willis JP, Desemone J, Bequette BW: Hypoglycemia prediction and detection using optimal estimation. *Diabetes Technol Ther* 7:3–14, 2005
17. Sparacino G, Zanderigo F, Corazza S, Maran A, Facchinetti A, Cobelli C: Glucose concentration can be predicted ahead in time from continuous glucose monitoring sensor time-series. *IEEE Trans Biomed Eng* 54:931–937, 2007
18. Kuure-Kinsey, Cutright R, Bequette BW: Computationally efficient neural predictive control based on a feedforward architecture. In *Proceedings of the American Control Conference,* Minneapolis, MN, IEEE, 2006, p. 2957–2962
19. Knobbe EJ, Buckingham B: The extended Kalman filter for continuous glucose monitoring. *Diabetes Technol Ther* 7:15–27, 2005
20. Dassau E, Bequette BW, Palerm CC, Buckingham BA, Gandrud LM, Doyle FJ III: Detection of a meal using continuous glucose monitoring (CGM), implications for model predictive control using a real-time CGM. *Diabetes* 56 (Suppl. 1):A23, 2007
21. The Diabetes Research in Children Network (DirecNet) Study Group: Impact of exercise on overnight glycemic control in children with type 1 diabetes mellitus. *J Pediatr* 147:528–534, 2005

Available online at www.sciencedirect.com
ScienceDirect
Journal of Process Control 18 (2008) 258–265
JOURNAL OF PROCESS CONTROL
www.elsevier.com/locate/jprocont

A run-to-run control strategy to adjust basal insulin infusion rates in type 1 diabetes

Cesar C. Palerm [a,b,c], Howard Zisser [c], Lois Jovanovič [c,b], Francis J. Doyle III [a,b,c,*]

[a] Department of Chemical Engineering, University of California Santa Barbara, Santa Barbara, CA 93106-5080, United States
[b] Biomolecular Science and Engineering Program, University of California Santa Barbara, Santa Barbara, CA 93106-9611, United States
[c] Sansum Diabetes Research Institute, 2219 Bath St., Santa Barbara, CA 93105-4321, United States

Received 19 January 2007; received in revised form 27 July 2007; accepted 27 July 2007

Abstract

Maintaining good glycemic control is a daily challenge for people with type 1 diabetes. Insulin requirements are changing constantly due to many factors, such as levels of stress and physical activity. The basal insulin requirement also has a circadian rhythm, adding another level of complexity. Automating the adjustment of insulin dosing would result in improved glycemic control, as well as an improved quality of life by significantly reducing the burden on the patient. Building on our previous success of using run-to-run control for prandial insulin dosing (a strategy adapted from the chemical process industry), we show how this same framework can be used to adjust basal infusion profiles. We present a mathematical model of insulin–glucose dynamics which we augment in order to capture the circadian variation in insulin requirements. Using this model, we show that the run-to-run framework can also be successfully applied to adjust basal insulin dosing.

Keywords: Type 1 diabetes; Run-to-run control; Basal infusion; Circadian variation

1. Introduction

Type 1 diabetes mellitus is a metabolic disease characterized by hyperglycemia (high blood glucose concentration), which is caused by an absolute deficiency of insulin secretion. There are an estimated 18 million people worldwide with the disease [1,2], and with a clear rising trend in its incidence [3]. People with type 1 diabetes fully depend on exogenous insulin, and managing their disease is a daily challenge.

Insulin dosing is divided into two regimens: basal and bolus insulin. The basal insulin covers the requirements in the absence of meals. The insulin bolus is associated with the carbohydrate content of meals (the insulin-to-carbohydrate ratio), and is calculated to offset the appearance of glucose from a meal. Both of these require adjustment over time.

The two main insulin delivery methods are continuous subcutaneous insulin infusion (CSII) pumps and multiple daily injections. CSII pumps are becoming the preferred method to deliver insulin, as CSII therapy significantly improves glycemic control [4]. Pumps have the advantage that basal insulin delivery can be set at different rates for distinct segments of the day (e.g., the Paradigm® pump, Medtronic MiniMed, Inc., Northridge, CA supports up to 48 segments). These segments are selected to accommodate changing insulin requirements due to the sleep–awake cycle and activity levels; a range of one to seven segments are common. The CSII pump is also used to deliver the meal-related insulin boluses.

Since the Diabetes Control and Complications Trial [5], the first large, prospective clinical trial, the accumulated

* Corresponding author. Address: Department of Chemical Engineering, University of California Santa Barbara, Santa Barbara, CA 93106-5080, United States.
E-mail addresses: palerm@ieee.org (C.C. Palerm), hzisser@sansum.org (H. Zisser), ljovanovic@sansum.org (L. Jovanovič), frank.doyle@icb.uscb.edu, doyle@engineering.ucsb.edu (F.J. Doyle III).

0959-1524/$ - see front matter © 2007 Elsevier Ltd. All rights reserved.
doi:10.1016/j.jprocont.2007.07.010

evidence is strong that blood glucose levels must be normalized in order to avoid the complications associated with diabetes [6]. Tight glucose control (i.e., as close to normal as possible) should be maintained for life in order to accrue the full benefits. Many factors influence the insulin dose requirements, including weight, physical condition, and stress levels. Due to the constantly changing insulin requirement, frequent blood glucose monitoring is mandated. Based on these glucose levels the insulin dosage must be modified, dietary changes implemented (such as alteration in the timing, frequency and content of the meals), and activity patterns changed.

Automating insulin delivery has, therefore, been an active field of research. There have been multiple algorithms proposed for closed-loop control of glycemia, including MPC [7–10], PD [11–13], PID [14–17], and H_∞ [18,19] – for a recent review of the literature in this area see [20]. All of these controllers are based on the assumption that a continuous glucose sensor is available, and although sensor technology has improved significantly over the last few years, it is still short of the reliability and accuracy required for commercial implementation of such a closed-loop system [20].

Even before continuous glucose monitoring, there have been substantial efforts to develop algorithms that use sparse blood glucose measurements. Most of these have evolved from within the medical community, and consist of heuristics based on clinical experience [21–29]. None of these algorithms use the newer monomeric insulin formulations, and most are aimed at multiple insulin injection therapy, rather than the use of CSII pumps.

We have previously tested a run-to-run control strategy to adjust the insulin-to-carbohydrate ratio based on post-meal blood glucose measurements [30–34], with the clinical results of the latest version of the algorithm being very encouraging [35]. The basal insulin infusion rate in these studies has been manually adjusted by the physician using retrospective continuous glucose monitoring [36].

Adjusting the basal infusion rates is not straightforward, as the effect of glucose appearance from a meal and the related insulin bolus make it difficult to distinguish if blood glucose changes are due to the basal or bolus dose. A common situation for many individuals is to have their basal rates set too low, and to compensate for the difference in the prandial bolus, which is not the best strategy. CSII pump manufacturers are introducing features to help subjects adjust their basal rates, but none provides rate adjustment recommendations.

In this paper we present the use of run-to-run control to adjust basal infusion rates using sparse blood glucose measurements. The performance measure used in our algorithm is derived, in part, from our clinical heuristic. The paper is organized as follows: we first introduce the clinical heuristic; we follow that with an overview of the run-to-run algorithm, and the derivation of the performance measure. We present simulation results of our control strategy, for which we introduce modifications to one of the previously published models of glucose kinetics in order to capture the circadian variation in insulin sensitivity and changes in physical activity. We conclude the paper with a discussion of the results.

2. Clinical adjustment of basal infusion rates

When starting a subject on CSII therapy, there are a number of steps the physician will follow [37]. The first one is to estimate the total insulin requirement, which depends on the subject's weight and other factors such as physical condition and stress. For a nominal subject under typical stress levels, this is calculated as

$$I = 0.6\frac{\mathrm{U}}{\mathrm{kg}\cdot\mathrm{day}}\cdot W\ \mathrm{kg} \tag{1}$$

where W is the subject's weight. Basal insulin requirements are roughly 50% of the total daily dose

$$B = 0.5I \tag{2}$$

The change in insulin sensitivity over the course of the day is driven by the circadian variation in hormone levels. Basal insulin needs are highest in the early morning, stable during the day, and lowest in the middle of the night, when hormones are at their nadir [37]. For this reason, a day is divided into four segments: midnight to 4:00, 4:00 to 10:00, 10:00 to 18:00 and 18:00 to midnight. For each segment the basal infusion rate is set to

$$B_{\text{infusion rate}} = \begin{cases} \frac{0.5B}{24\text{h}} & \text{midnight–4:00} \\ \frac{1.5B}{24\text{h}} & \text{4:00–10:00} \\ \frac{1.0B}{24\text{h}} & \text{10:00–18:00} \\ \frac{1.0B}{24\text{h}} & \text{18:00–midnight} \end{cases} \tag{3}$$

as the initial estimate. From this starting point, it is necessary to fine-tune the infusion rates based on the subject's response. Initially, the same basal rate is used for the third and fourth segments. This is to provide a transition point from the outset at a time of the day when some people may have a drastic change in physical activity levels. Based on the person's actual patterns the physician can choose different ways of segmenting the day, but in most cases these four suffice.

In order to optimize the basal rates, the subject wears a continuous glucose monitoring system for a period of three days. Such a system records the blood glucose concentration every five minutes, thus providing a full history of the glucose changes. During this time they skip a meal each day, with the purpose of obviating the effects of the prandial insulin bolus and the glucose appearing from the corresponding meal. Basal infusion rates are adjusted to target a fasting blood glucose of 90 mg/dL. The process is repeated as necessary until fasting levels, in the absence of a meal, are at the target level [36].

Fig. 1 shows a two-day sequence before the basal rate is adjusted, with the subject skipping breakfast on the second day. The hyperglycemic excursion during the course of the

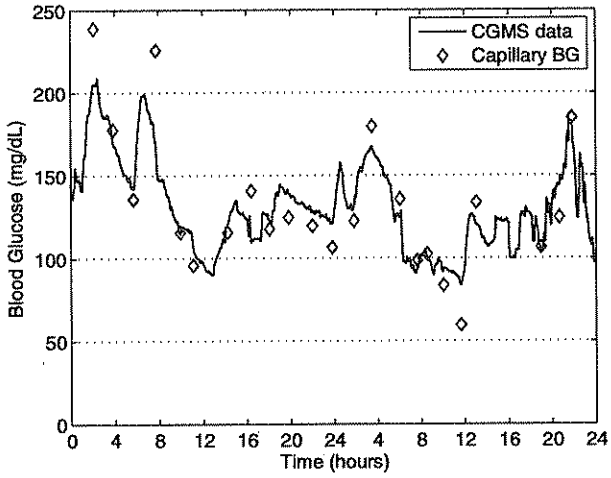

Fig. 1. Two-day sequence (starting at midnight) of CGMS blood glucose data before the adjustment of basal rates; the subject skipped breakfast on the second day. The hyperglycemic excursion during the night indicates that the basal infusion rate for this period is too low, while the morning segment of the second day is correct. Diamonds indicate the capillary blood glucose calibration measurements.

night indicates that the overnight basal infusion rate is too low (midnight–4:00), while the morning segment (4:00–10:00) is within the clinically acceptable range. Fig. 2, first day, shows the overnight segment, and again no breakfast in the morning. This figure also shows the effects of dinner and the three meals on the following day, highlighting why manual adjustment requires meals to be skipped.

Once these basal infusion rates are set, they require periodic re-adjustment. Sometimes a person will realize that their blood glucose levels have not been under control, and at that point will seek assistance in adjusting their dosing. In the meantime, they have gone for several days with less than optimal glycemic control.

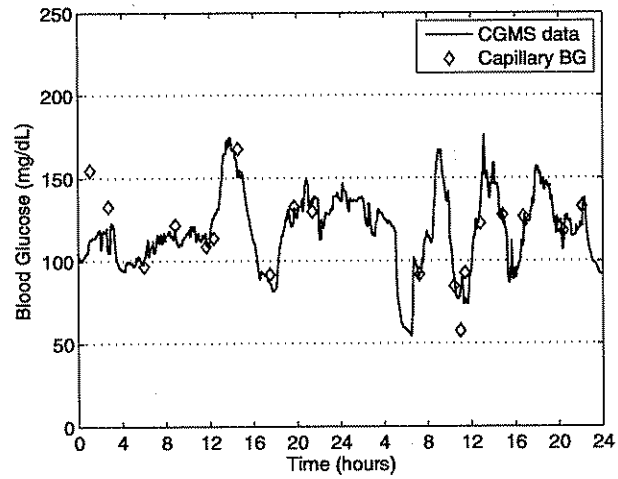

Fig. 2. Two-day sequence (starting at midnight) of CGMS blood glucose data after the adjustment of basal rates; the subject skipped breakfast on first day. Nighttime and morning basal rates are correctly set. Diamonds indicate the capillary blood glucose calibration measurements.

3. Run-to-run control

Taking the clinical heuristic as a starting point, we have adapted a run-to-run control algorithm to adjust basal insulin infusion rates using only sparse blood glucose measurements. The strategy is adapted from the chemical process industry [38], in the same spirit as the insulin-to-carbohydrate ratio adjustment algorithms previously developed [30–35].

The standard run-to-run control algorithm [38] consists of the following steps:

(1) Parameterize the input profile for run k, $u_k(t)$, as $\mathscr{U}(t, v_k)$. Also consider a sampled version, ψ_k, of the output $y_k(t)$, such that it has the same dimension as the manipulated variable vector v_k. Thus we have

$$\psi_k = F(v_k)$$

(2) Choose an initial guess for v_k (when $k = 1$).
(3) Complete the run using the input $u_k(t)$ corresponding to v_k. Determine ψ_k from the measurements $y_k(t)$.
(4) Update the input parameters as

$$v_{k+1} = v_k + K(\psi^r - \psi_k)$$

where K is an appropriate gain matrix and ψ^r represents the reference values to be attained. Increment k for the next run, and repeat steps 3–4 until convergence.

The algorithm allows for individualizing the number of segments and the corresponding timing. Using the run-to-run strategy, each day is considered a run. For the current day, a performance measure is calculated for each segment and then used to automatically adjust the amount of insulin for each corresponding segment on the following day. Because the algorithm adjusts based on the glucose measurements at the end of a segment, the number of segments dictates the number of glucose measurements required. These measurements drive the algorithm to maintain, increase or decrease the amount of insulin infused for the corresponding segment on the following day. This dose correction process is designed to be independent of physician or subject intervention.

In the absence of meals or other events affecting blood glucose levels (e.g., exercise), the basal insulin infusion rate must keep the subject's blood glucose in the normal range of 70–110 mg/dl. If the amount of insulin infused over the time segment is too low, the blood glucose level will rise above the desired range. If the basal dose is too large, it will tend to lower blood glucose into the hypoglycemic range.

Given that the number of blood glucose measurements has to be minimized for the strategy to be practical, these have to be taken at strategic times in relation to the segments chosen. Fig. 3 illustrates this. For segment one, adjustment is made using measurements at start and end of the segment (BG_1 and BG_2). Segment two is adjusted with the measurement right before breakfast (BG_3),

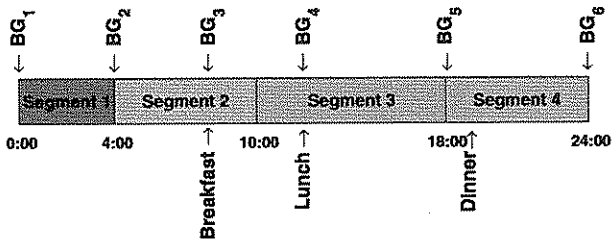

Fig. 3. Nominal basal segments for a day, indicating meal and blood glucose measurement times.

in order to avoid the prandial glucose excursion, and the measure at the start of the segment (BG_2). In the case of segment three, the first measurement (BG_4) is delayed to the start of lunch to avoid effects from breakfast; this also minimizes the number of fingersticks needed. Finally, for segment four, the first measurement is not delayed, as BG_5 is also used for the end of segment three; the ending measurement (BG_6) is also (BG_1) for the following day.

Regardless of the blood glucose level coming into a segment, the perfect basal insulin dose should keep this level constant during the segment. The deviation

$$\Delta G = G_{\text{end of segment } i} - G_{\text{start of segment } i} \tag{4}$$

where G is the corresponding blood glucose measurement, is the performance measure that is used as the controlled variable (ψ). The controlled variable vector (assuming four segments) is then

$$\psi_k = [\Delta G_1 \quad \Delta G_2 \quad \Delta G_3 \quad \Delta G_4]^{\mathrm{T}} \tag{5}$$

where k is the current day.

Using the above formulation, there exist multiple "perfect" basal doses, which will keep blood glucose at a different target over the segment. Because of this, a second controlled variable vector is set to

$$\varphi_k = [G_{1_{\text{avg}}} \quad G_{2_{\text{avg}}} \quad G_{3_{\text{avg}}} \quad G_{4_{\text{avg}}}]^{\mathrm{T}} \tag{6}$$

where

$$G_{i_{\text{avg}}} = 0.5(G_{\text{start of segment } i} + G_{\text{end of segment } i}) \tag{7}$$

such that the desired fasting blood glucose can be targeted.

The input parameters (the basal infusion rate for each segment) are then updated using

$$v_{k+1} = v_k + K_1(\psi^r - \psi_k) + K_2(\varphi^r - \varphi_k) \tag{8}$$

where K_1 and K_2 are gain matrices, and $\psi^r = 0$ mg/dl and $\varphi^r = 80$ mg/dl are the reference target values. The new doses are implemented the following day, and the procedure repeated.

In cases when there are too many complicating events to capture the effect of the basal rate, the adjustment for that day can be omitted. As the initial guess for v_k at $k = 0$, the same settings as in the manual adjustment procedure (3) can be used.

Given that the insulin requirement to maintain blood glucose constant for a given segment is independent of the other segments, it is appropriate for the gain matrix K_1 to be designed as a diagonal matrix. For the same reasons, the gain matrix K_2 is also designed as a diagonal matrix. The tuning for each gain matrix can then be done independently for each segment, allowing for the possibility that different levels of aggressiveness in the adjustments be allowed for different times of day.

The algorithm (8) is guaranteed to yield a single optimum solution. Because the start of a segment coincides with the end of the previous segment, this provides a sufficient constraint to guarantee a unique solution at steady-state, which is a blood glucose at the desired reference value (see Appendix for proof).

4. Simulation model

Currently, there are no published models of insulin–glucose dynamics that incorporate the circadian variation of insulin sensitivity, nor the changing insulin requirements due to changing levels of physical activity. Since the run-to-run control strategy proposed is meant to compensate for precisely these factors, one of the current models was modified to incorporate an approximation of such effects.

The model used is that of Hovorka et al. [7], replacing the subcutaneous insulin infusion model with that presented in [39]. The core of the model consists of two compartments for glucose (plasma and tissue) and one compartment for plasma insulin. The model divides the action of insulin on glucose kinetics into three additional components (x_1 for the effects of insulin on glucose distribution/transport, x_2 for glucose disposal, and x_3 for endogenous glucose production), which are described by

$$\dot{x}_1 = -k_{a1}x_1(t) + k_{b1}I(t) \tag{9a}$$

$$\dot{x}_2 = -k_{a2}x_2(t) + k_{b2}I(t) \tag{9b}$$

$$\dot{x}_3 = -k_{a3}x_3(t) + k_{b3}I(t) \tag{9c}$$

where the parameters k_{b1}, k_{b2}, and k_{b3} correspond to the insulin sensitivity of each mechanism of action of insulin, and $I(t)$ is the plasma insulin concentration.

The circadian change in insulin sensitivity has been modeled by introducing a modulating gain which affects all sensitivities equally. This is introduced by replacing $I(t)$ in Eq. (9) with $I'(t)$ as given by

$$I'(t) = k_m(t)I(t) \tag{10}$$

where the modulating gain $k_m(t)$ is given, in the Lapalce domain, by

$$k_m(s) = \frac{e^{-\tau_d s}}{(15s+1)(s+1)}k_p(s) \tag{11}$$

with the input $k_p(t)$ being a step profile corresponding to the desired gain for each segment. Given that the model is now time-varying with respect to time of day, $t = 0$ is set to correspond to midnight. The dynamics are set according to expected behavior based on what is known of the underlying physiology. The delay introduced in the

Table 1
For the standard segments of the day, 13 cases were created based on subject data that had their basal rates manually optimized in a previous study [36]

Case	Segment 1	Segment 2	Segment 3	Segment 4
1	0.91	1.52	1.52	1.60
2	0.73	1.02	0.73	0.87
3	0.69	1.37	0.91	1.26
4	0.72	1.44	1.04	0.96
5	0.29	0.87	0.87	0.87
6	0.79	1.35	0.79	1.13
7	0.99	1.48	1.38	1.58
8	1.08	2.27	1.95	2.38
9	0.89	0.98	0.71	0.53
10	0.29	0.91	0.29	0.34
11	0.60	1.42	1.20	1.05
12	0.53	1.60	1.00	0.71
13	0.87	1.03	0.87	0.87

input (τ_d) is relative to when the infusion profile changes, as the change in sensitivity is known to start earlier. This parameter is optimized such that the desired infusion profile maintains the blood glucose concentration as close to 80 mg/dl as possible, in the absence of any simulated meals.

A set of cases was created from actual subject pump infusion profiles. We obtained 13 manually optimized basal infusion profiles from a group of subjects [36]. Table 1 shows the multipliers for each segment assuming that the basal insulin dose requirement has been calculated according to the clinical guidelines (Eq. (2)). In all cases the timing for the segments is the same as the nominal (i.e., midnight–4:00, 4:00–10:00, 10:00–18:00 and 18:00–midnight). The delay τ_d was optimized independently for each case. The median delay was 11 min, with a range of 10.4–16.7 min.

One of the limitations of the Hovorka et al. [7] model is the component that describes the absorption of glucose from the consumption of a mixed meal. In daily living conditions, with the correct bolus dose of insulin to cover a meal, the blood glucose concentration is expected to return to basal levels within two to three hours after the start of the meal [40,31]. The dynamics of the model for this case are much slower than this, resulting in extremely long settling times that are not physiologically correct. For this reason, the time constants for the absorption part of the model have been modified such that the settling time is more consistent with the subject data. This results in an initial rate of change that is too aggressive, but this will not affect the results of the simulations presented, as no blood glucose measurements are used within the first two hours of any postprandial period. The parameter in the Hovorka et al. [7] model that was changed is $t^2_{\max,G}$, from a value of 40 min to a value of 5 min.

5. Results

Fig. 4 shows the simulation over a day using the correct basal and prandial dosing, which illustrates the adjusted timing of the blood glucose measurements in order to minimize the effects of the meals. For all cases, the algorithm is initialized using the clinical heuristics (Eq. (3)), with the total basal dose calculated from the actual requirements according to the model (rounded down to the nearest whole unit of insulin). Meals are assumed to be the same from day to day, and the dose of the prandial insulin bolus to be correctly matched. There are constraints on the rate of change of the dosing for any given segment from one day to the next, with a 20% maximum increase and a 30% maximum decrease.

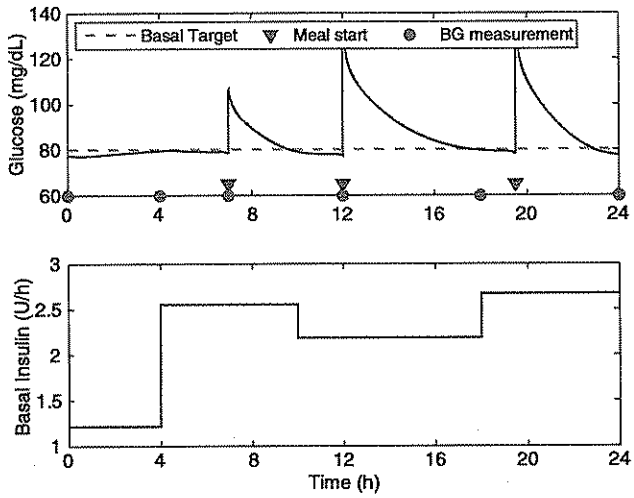

Fig. 4. Blood glucose response over a day with the corresponding basal infusion profile. The circles indicate the timepoints at which blood glucose measurements are taken for use by the algorithm, and the triangles indicating the starting time of meals.

Clinically, it is desirable to have the basal infusion rates converge within a time frame of seven days. Therefore, the gains of the run-to-run controller were manually tuned to meet this specification. For the simulations, the gain matrices were set to be $K_j = k_j I$, $j = 1, 2$, where k_j is a scalar, and I the identity matrix, which sets the same tuning for all segments. The gains were set to $k_1 = 0.01$ and $k_2 = 0.0067$. Setting k_2 to be smaller than k_1 is desirable, as converging to the desired blood glucose level is a secondary objective to maintaining blood glucose steady throughout the corresponding segment.

For the 13 cases, the algorithm was considered to have converged once the basal profile was within 10% of the actual profile for all four segments. On average, the algorithm converged in 6.3 days, with a standard deviation of 2.1 days. There is one case (number 10) which does not converge to within 10%, but does so within 15%. With the 15% metric, all cases converge, with an average of 5.1 days and a standard deviation of 2.3 days. Case 10 is a particularly challenging scenario, as the subject has a very high insulin sensitivity, except during the 4:00–10:00 segment, in which the insulin requirement is 2.7–3.1 times higher than for the other segments. Over all the cases, the constraints are rarely active, with the exception of case 10. Overall, the median for the number of times a

constraint is active over 15 days of simulation is one time, with a range of 0–14.

Fig. 5 shows the simulation for a representative case (number eight) over 10 days. This case takes five days to converge, and has no active constraints. Fig. 6 shows day seven of this run; this is the same profile as the perfect day example shown in Fig. 4. The reason the profile does not converge perfectly to the underlying profile is due in large measure to the remaining effects of the meals, which are not completely eliminated even after several hours.

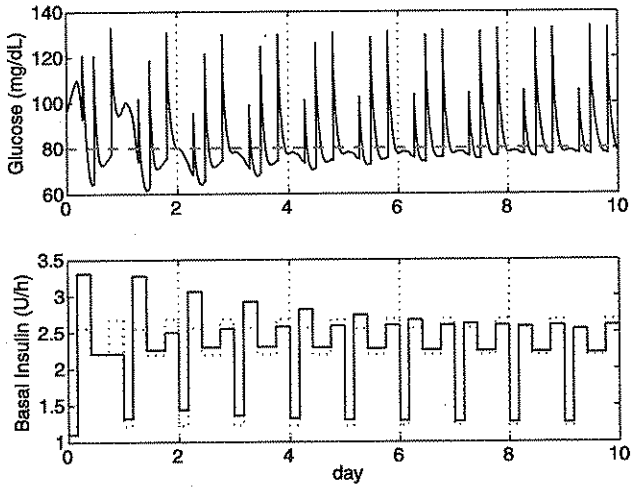

Fig. 5. Blood glucose response over 10 days with the corresponding basal infusion profile for case eight. The dotted line in the insulin plot indicates the optimal basal infusion profile. Initial basal rates are set according to the clinical heuristics, with segment one slightly underdosed, segment two is overdosed, segment three is very close to target, and segment four is underdosed. These settings result in periods of hyper- and hypoglycemia, with levels converging to clinically acceptable levels by the fifth day.

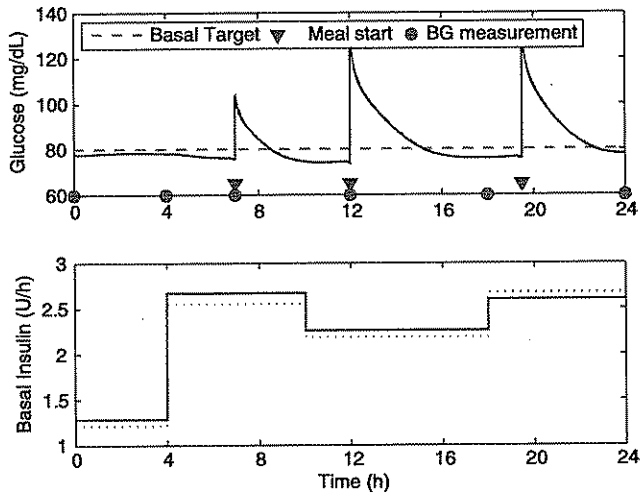

Fig. 6. Blood glucose response for day seven of the simulation run for case eight. The dotted line in the insulin plot indicates the optimal basal infusion profile. The blood glucose profile shows good glycemic control over the day, with the basal infusion rates being very close to the optimal rates.

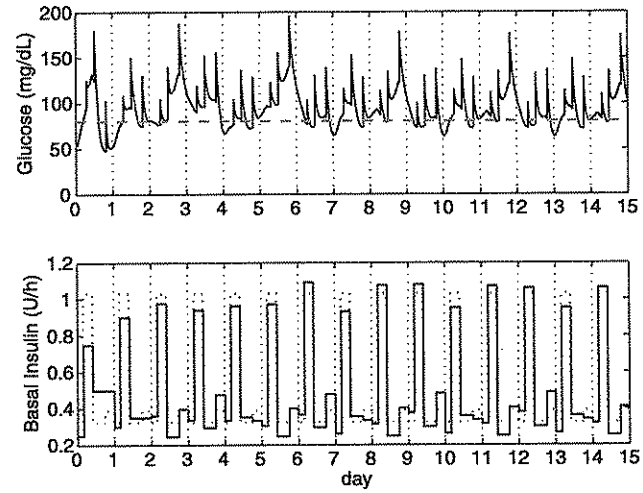

Fig. 7. Blood glucose response over 15 days for the worst case (number 10). The initial setting based on the clinical heuristics are significantly off, with the subject showing high insulin sensitivity in all but the morning segment, which has significantly higher insulin requirements. The dotted line in the insulin plot indicates the optimal basal infusion profile.

Case 10 is shown in Fig. 7 for a simulation run of 15 days. Even small changes in the basal profile from one day to the next, compounded with the deviations introduced by the meals, introduce large changes in the blood glucose response. In this case, an unconstrained design would drive the subject to frequent hypoglycemia. Detuning the controller would alleviate this issue, but at the expense of a very sluggish response for the remaining 12 cases.

6. Conclusions

Adjusting basal and prandial insulin dosing is a daily chore for people with type 1 diabetes. The success in developing an algorithm to adjust prandial insulin dosing based on medical expertise [31,35,41] has further motivated the development of a similar strategy for basal insulin dosing.

A major hurdle has been the lack of a mathematical model that incorporates the dynamics associated with the circadian changes in basal insulin requirements. We presented a first approximation of such a model by using the manually optimized profiles of a group of subjects. Although not based on the underlying physiology, it serves the purpose of challenging the algorithm appropriately.

Using only five, properly timed, blood glucose measurements, we have shown that the proposed run-to-run algorithm can successfully adjust basal infusion rates for the nominal four segments. Different daily segments can be easily accommodated by the algorithm, requiring only the proper timing for the blood glucose measurements. Being able to make dose adjustment decisions even in the presence of meals is a significant improvement over current

clinical strategies. Even with the error introduced by the tail end of the meal response, basal rates converge in less than a week on average.

In the clinical testing of the algorithm the additional challenge will be that the meal-related insulin dose might not be correct either. To avoid this potential confounding factor, initial testing can be done by skipping meals as in the manual adjustment protocol. Eventually, a strategy that combines the adjustment of basal and bolus insulin dosing will be required. Appropriate heuristics will need to be incorporated, as the interplay between these two components of insulin therapy are not negligible.

The benefits of tight glycemic control are significant, and a run-to-run framework for the adjustment of basal and bolus insulin dosing can be an important tool in accomplishing this goal.

Acknowledgement

This work was supported by the National Institutes of Health, Grants R01-DK068706 and R01-DK068663.

Appendix A

Without loss of generality, we can assume the four standard segments, with the initial and ending blood glucose measurements coinciding for the end of a segment and the beginning of the next one. Thus segment one uses G_{1_k} and G_{2_k}, segment two uses G_{2_k} and G_{3_k} and so on.

To simplify the notation, we use deviation variable form, thus

$$G_{id_k} = G_{i_k} - \varphi^r, \quad i = 1 \ldots 5 \tag{A.1}$$

and the update law in deviation variable form, with the references being zero, is

$$v_{k+1} = v_k + K_1(-\psi_{d_k}) + K_2(-\varphi_{d_k}) \tag{A.2}$$

and without loss of generality, we can assume $K_j = k_j I$, $j = 1, 2$, where k_j is a scalar, and I the identity matrix.

We know that once steady-state is reached, there will be no further corrections, thus $v_{k+1} = v_k$. For now drop the k subscript as we refer to the same day. Looking at just the first segment, we have

$$k_1(G_{1d} - G_{2d}) = \frac{k_2}{2}(G_{1d} + G_{2d}) \tag{A.3}$$

$$G_{2d} = \frac{2k_1 - k_2}{2k_1 + k_2} G_{1d} \tag{A.4}$$

and let

$$f = \frac{2k_1 - k_2}{2k_1 + k_2} \tag{A.5}$$

then $G_{2d} = fG_{1d}$. Similarly, we have

$$G_{3d} = f^2 G_{1d} \tag{A.6}$$

$$G_{4d} = f^3 G_{1d} \tag{A.7}$$

$$G_{5d} = f^4 G_{1d} \tag{A.8}$$

Since $G_{5d} = G_5 - \varphi^r$ and $G_{1d} = G_1 - \varphi^r$, we have

$$G_{5d} = f^4 G_{1d} \tag{A.9}$$

$$G_5 - \varphi^r = f^4(G_1 - \varphi^r) \tag{A.10}$$

$$G_5 = f^4 G_1 + (1 - f^4)\varphi^r \tag{A.11}$$

but G_5 is the same as G_1 on the following day, thus

$$G_{1_{k+1}} = f^4 G_{1_k} + (1 - f^4)\varphi^r \tag{A.12}$$

and if we are indeed in steady-state, then $G_{1_{k+1}} = G_{1_k}$, thus

$$G_1 = f^4 G_1 + (1 - f^4)\varphi^r \tag{A.13}$$

$$G_1 = \varphi^r \tag{A.14}$$

thus we have only one solution, which holds for the other segment endpoints as well. It is straightforward to show that this still holds true when the measurements do not coincide, as illustrated in the case shown in Fig. 3.

References

[1] L. Eiselein, H.J. Schwartz, J.C. Rutledge, The challenge of type 1 diabetes mellitus, ILAR J. 45 (3) (2004) 231–236.
[2] World Health Organization, Diabetes (fact sheet no. 312), September 2006. WHO Web site: <http://www.who.int/mediacentre/factsheets/fs312/en/> (Retrieved 11.01.07).
[3] E.A.M. Gale, Spring harvest? Reflections on the rise of type 1 diabetes, Diabetologia 48 (12) (2005) 2445–2450.
[4] J. Weissberg-Benchell, J. Antisdel-Lomaglio, R. Seshadri, Insulin pump therapy: a meta-analysis, Diabetes Care 26 (2003) 1079–1087.
[5] Diabetes Control and Complications Trials Research Group, The effect of intensive treatment of diabetes on the development and progression of long-term complications in insulin-dependent diabetes mellitus, N. Engl. J. Med. 329 (1993) 977–986.
[6] W.T. Cefalu, Glycemic control and cardiovascular disease – should we reassess clinical goals? N. Engl. J. Med. 353 (25) (2005) 2707–2709.
[7] R. Hovorka, V. Canonico, L.J. Chassin, U. Haueter, M. Massi-Benedetti, M.O. Federici, T.R. Pieber, H.C. Schaller, L. Schaupp, T. Vering, M.E. Wilinska, Nonlinear model predictive control of glucose concentration in subjects with type 1 diabetes, Physiol. Meas. 25 (4) (2004) 905–920.
[8] S.M. Lynch, B.W. Bequette, Model predictive control of blood glucose in type I diabetics using subcutaneous glucose measurements, in: Proceedings of the American Control Conference, 2002, pp. 4039–4043.
[9] R.S. Parker, F.J. Doyle III, N.A. Peppas, A model-based algorithm for blood glucose control in type I diabetic patients, IEEE Trans. Biomed. Eng. 46 (2) (1999) 148–157.
[10] H.C. Schaller, L. Schaupp, M. Bodenlenz, M.E. Wilinska, L.J. Chassin, P. Wach, T. Vering, R. Hovorka, T.R. Pieber, On-line adaptive algorithm with glucose prediction capacity for subcutaneous closed loop control of glucose: evaluation under fasting conditions in patients with type 1 diabetes, Diabet. Med. 23 (1) (2006) 90–93.
[11] Y. Matsuo, S. Shimoda, M. Sakakida, K. Nishida, T. Sekigami, S. Ichimori, K. Ichinose, M. Shichiri, E. Araki, Strict glycemic control in diabetic dogs with closed-loop intraperitoneal insulin infusion algorithm designed for an artificial endocrine pancreas, J. Artif. Organs 6 (1) (2003) 55–63.
[12] T. Sekigami, S. Shimoda, K. Nishida, Y. Matsuo, S. Ichimori, K. Ichinose, M. Shichiri, M. Sakakida, E. Araki, Comparison between closed-loop portal and peripheral venous insulin delivery systems for an artificial endocrine pancreas, J. Artif. Organs 7 (2) (2004) 91–100.
[13] S. Shimoda, K. Nishida, M. Sakakida, Y. Konno, K. Ichinose, M. Uehara, T. Nowak, M. Shichiri, Closed-loop subcutaneous insulin infusion algorithm with a short-acting insulin analog for long-term

clinical application of a wearable artificial endocrine pancreas, Front. Med. Biol. Eng. 8 (3) (1997) 197–211.
[14] G. Marchetti, M. Barolo, L. Jovanovic, H. Zisser, D. Seborg, An improved pid switching control strategy for type 1 diabetes, in: Engineering in Medicine and Biology Society, 2006. EMBS'06. 28th Annual International Conference of the IEEE, 2006, pp. 5041–5044.
[15] A.E. Panteleon, M. Loutseiko, G.M. Steil, K. Rebrin, Evaluation of the effect of gain on the meal response of an automated closed-loop insulin delivery system, Diabetes 55 (7) (2006) 1995–2000.
[16] G.M. Steil, A.E. Panteleon, K. Rebrin, Closed-loop insulin delivery-the path to physiological glucose control, Adv. Drug Deliv. Rev. 56 (2) (2004) 125–144.
[17] G.M. Steil, M.F. Saad, Automated insulin delivery for type 1 diabetes, Curr. Opin. Endocrinol. Diabetes 13 (2) (2006) 205–211.
[18] R.S. Parker, F.J. Doyle III, J.H. Ward, N.A. Peppas, Robust H_∞ glucose control in diabetes using a physiological model, AIChE J. 46 (12) (2000) 2537–2549.
[19] E. Ruiz-Velzquez, R. Femat, D.U. Campos-Delgado, Blood glucose control for type I diabetes mellitus: A robust tracking H_∞ problem, Control Eng. Pract. 12 (9) (2004) 1179–1195.
[20] R. Hovorka, Continuous glucose monitoring and closed-loop systems, Diabet. Med. 23 (1) (2006) 1–12.
[21] J. Beyer, J. Schrezenmeir, G. Schulz, T. Strack, E. Kstner, G. Schulz, The influence of different generations of computer algorithms on diabetes control, Comput. Methods Programs Biomed. 32 (3–4) (1990) 225–232.
[22] L.H. Chanoch, L. Jovanovic, C.M. Peterson, The evaluation of a pocket computer as an aid to insulin dose determination by patients, Diabetes Care 8 (2) (1985) 172–176.
[23] F. Chiarelli, S. Tumini, G. Morgese, A.M. Albisser, Controlled study in diabetic children comparing insulin-dosage adjustment by manual and computer algorithms, Diabetes Care 13 (10) (1990) 1080–1084.
[24] L. Jovanovic, C.M. Peterson, Home blood glucose monitoring, Compr. Ther. 8 (1) (1982) 10–20.
[25] A. Peters, M. Rübsamen, U. Jacob, D. Look, P.C. Scriba, Clinical evaluation of decision support system for insulin-dose adjustment in IDDM, Diabetes Care 14 (10) (1991) 875–880.
[26] C.M. Peterson, L. Jovanovic, L.H. Chanoch, Randomized trial of computer-assisted insulin delivery in patients with type I diabetes beginning pump therapy, Am. J. Med. 81 (1) (1986) 69–72.
[27] A. Schiffrin, M. Mihic, B.S. Leibel, A.M. Albisser, Computer-assisted insulin dosage adjustment, Diabetes Care 8 (6) (1985) 545–552.
[28] J. Schrezenmeir, K. Dirting, P. Papazov, Controlled multicenter study on the effect of computer assistance in intensive insulin therapy of type 1 diabetics, Comput. Methods Programs Biomed. 69 (2) (2002) 97–114.
[29] J.S. Skyler, D.L. Skyler, D.E. Seigler, M.J. O'Sullivan, Algorithms for adjustment of insulin dosage by patients who monitor blood glucose, Diabetes Care 4 (2) (1981) 311–318.
[30] C.L. Owens, H. Zisser, L. Jovanovic, B. Srinivasan, D. Bonvin, F.J. Doyle III, Run-to-run control of blood glucose concentrations for people with type 1 diabetes mellitus, IEEE Trans. Biomed. Eng. 53 (6) (2006) 996–1005.
[31] C.C. Palerm, H. Zisser, W.C. Bevier, L. Jovanovič, F.J. Doyle III, Prandial insulin dosing using run-to-run control: application of clinical data and medical expertise to define a suitable performance metric, Diabetes Care 30 (5) (2007) 1131–1136.
[32] C.C. Palerm, H. Zisser, L. Jovanovic, F.J. Doyle III, Flexible run-to-run strategy for insulin dosing in type 1 diabetic subjects, in: Proceedings of the International Symposium on Advanced Control of Chemical Processes, Gramado, Brazil, 2006, pp. 521–526.
[33] C.C. Palerm, H. Zisser, L. Jovanovič, F.J. Doyle III, A run-to-run framework for prandial insulin dosing: handling real-life uncertainty, Int. J. Robust Nonlin. 17 (13) (2007) 1194–1213.
[34] H. Zisser, L. Jovanovic, F. Doyle III, P. Ospina, C. Owens, Run-to-run control of meal-related insulin dosing, Diabetes Technol. Ther. 7 (1) (2005) 48–57.
[35] C.C. Palerm, H. Zisser, W. Bevier, F.J. Doyle, III, L. Jovanovič, Improved clinical outcome using sparse measurements and run-to-run control for prandial insulin dosing, in: Diabetes Technology Meeting, Atlanta, GA, USA, 2006, p. A127.
[36] H. Zisser, W.C. Bevier, L. Jovanovič, Restoring euglycemia in the basal state using continuous glucose monitoring in subjects with type 1 diabetes mellitus, Diabetes Technol. Ther., in press.
[37] L. Jovanovic, Insulin therapy and algorithms for treating type 1 diabetes mellitus, in: Optimizing insulin therapy in patients with diabetes, CME Activity jointly sponsored by Washington Hospital Center and MedStar Research Institute, 2002, pp. 13–19.
[38] B. Srinivasan, C.J. Primus, D. Bonvin, N.L. Ricker, Run-to-run optimization via control of generalized constraints, Control Eng. Pract. 9 (8) (2001) 911–919.
[39] M.E. Wilinska, L.J. Chassin, H.C. Schaller, L. Schaupp, T.R. Pieber, R. Hovorka, Insulin kinetics in type-1 diabetes: continuous and bolus delivery of rapid acting insulin, IEEE Trans. Biomed. Eng. 52 (1) (2005) 3–12.
[40] W.C. Bevier, H. Zisser, C.C. Palerm, D.A. Finan, D.E. Seborg, F.J. Doyle III, A. Okada Wollitzer, L. Jovanovič, Calculating the insulin to carbohydrate ratio using the hyperinsulinemic euglycemic clamp – a novel use for a proven technique, Diabetes Metab. Res. Rev. 23 (6) (2007) 472–478.
[41] C.C. Palerm, H. Zisser, W.C. Bevier, L. Jovanovič, F.J. Doyle III, Prandial insulin dosing using run-to-run control: application of clinical data and medical expertise to define a suitable performance metric, in: N.A. Peppas, A.S. Hoffman, T. Kanamori, K. Tojo (Eds.), Advances in Medical Engineering, Drug Delivery Systems and Therapeutic Systems, AIChE, New York, NY, USA, 2006, pp. 115–119.

Journal of Diabetes Science and Technology
Volume 1, Issue 6, November 2007

SYMPOSIUM

Glucose Estimation and Prediction through Meal Responses Using Ambulatory Subject Data for Advisory Mode Model Predictive Control

Rachel Gillis,[1] Cesar C. Palerm, Ph.D.,[1,3,4] Howard Zisser, M.D.,[2] Lois Jovanovič, M.D.,[2,3] Dale E. Seborg, Ph.D.,[1] and Francis J. Doyle, III, Ph.D.[1,3]

Abstract

Background:

A primary challenge for closed-loop glucose control in type 1 diabetes mellitus (T1DM) is the development of a control strategy that will be applicable during all daily activities, including meals, stress, and exercise. A model-based control algorithm requires a mathematical model that has the simplicity for online glucose prediction, yet retains the complexity necessary to cope with variations in insulin sensitivities and carbohydrate ingestion.

Methods:

A modified Bergman minimal model was linearized for Kalman filter (KF) state estimation on data from T1DM subjects, and multiple methods of parameter augmentation were developed for online adaptation. In addition, model deterioration for glucose prediction was assessed to determine an appropriate prediction horizon for model predictive control (MPC). Furthermore, MPC strategies were validated using advisory mode simulations.

Results:

Twenty days of continuous glucose data, which included 97 meals, were evaluated for three subjects. A constant parameter minimal model was used to predict glucose levels for normal days with meal announcement and with a maximum prediction horizon of approximately 45 minutes. In order to attain this prediction horizon in the absence of meal announcement, parameter adaptation was necessary to capture the glucose disturbance. Evaluation of advisory mode MPC permitted effective tuning for a moderately aggressive controller that responded well to meal disturbances.

continued →

Author Affiliations: [1]Department of Chemical Engineering, University of California, Santa Barbara, California, [2]Sansum Diabetes Research Institute, Santa Barbara, California, [3]Biomolecular Science and Engineering Program, University of California, Santa Barbara, California, and [4]Current Affiliation: Medtronic Diabetes

Abbreviations: (CGMS) continuous glucose monitoring systems, (KF) Kalman filter, (MPC) model predictive control, (MRAD) median relative absolute difference, (T1DM) type 1 diabetes mellitus

Keywords: artificial pancreas, model predictive control, patient model, type 1 diabetes

Corresponding Author: Francis J. Doyle, III, Ph.D, Department of Chemical Engineering, University of California, Santa Barbara, Santa Barbara, CA 93106-9611; email address *doyle@engineering.ucsb.edu*

Abstract cont.

Conclusions:

Estimation and prediction of glucose were accomplished using a KF based on a modified Bergman model. For a model with no meal announcement, parameter adaptation provided the means for closed-loop implementation. This state estimation and model validation scheme established the necessary framework for advisory mode MPC.

J Diabetes Sci Technol 2007;1(6):825-833

Introduction

Diabetes is a disease characterized by the improper production of insulin or insulin-mediated glucose disposal. This insulin deficiency results in hyperglycemia, as the hormone controls the metabolism of ingested carbohydrates and the glucose generated from gluconeogenic amino acids in protein. Complications associated with diabetes include high blood pressure, kidney disease, heart disease, and blindness, which result from the inability to maintain tight glucose control.[1–3] The severity of these long-term complications can be reduced through the regulation of blood glucose levels.[4] Currently, there is no cure for type 1 diabetes mellitus (T1DM), and although the only treatment is through insulin therapy, a healthy life can be sustained when normoglycemia is achieved and maintained.

Many T1DM subjects use manually controlled insulin pumps to administer meal-time insulin boluses and correction insulin boluses, but the insulin pump can be preprogrammed to deliver basal insulin. Continuous glucose monitoring systems (CGMS) allow subjects with diabetes to track absolute blood glucose concentrations and trends in real time.[5] The two technologies of continuous glucose sensing and continuous insulin infusion presently work independently, but much research has been focused on developing a controller that will combine these two technologies for closed-loop glucose control and eliminate the need for the individual with T1DM from insulin dosage decision making in this control loop.

Model predictive control (MPC) and state estimation have been the foundation of simulated studies of glucose control, but only a few clinical studies have been reported.[6–11] Parker *et al.*[6–8] developed several MPC schemes, including controllers with state estimation, which were tested on the 19-state Sorensen model.[12] Lynch and Bequette[10] demonstrated plant-model mismatch with linear Kalman filter (KF) state estimation and designed a model predictive controller based on the Bergman "minimal" model.[13] The discrete state space model used by Lynch and Bequette[10] included an augmented input disturbance term. Control performance was tested in a subject simulated by the higher order Sorensen model.[12] Hovorka and colleagues[11] experimentally demonstrated the capabilities of a complex, nonlinear MPC strategy for T1DM subjects through fasting conditions; several model parameters were adapted online using a Bayesian approach.

The focus of this article was to develop a state estimation method that implements a simple model capable of online adaptation to capture glucose–insulin dynamics in actual data generated in a clinical setting. This estimation scheme was tested on a total of 97 meal responses for three T1DM subjects and model prediction degradation as the prediction horizon increased. Model updating through parameter augmentation is presented as a method for online adaptation. Additionally, advisory mode MPC for 20 days of ambulatory subject data validates the MPC strategy.

Modeling

A number of physiological, compartmental models have been developed to describe insulin–glucose kinetics, ranging from simple three-state models to comprehensive models that include transport and diffusion rates.[12–17] Two models are considered in this article: the so-called Bergman and Hovorka models.

Bergman *et al.*[13] developed the "minimal model" to characterize plasma insulin and plasma glucose dynamics during an intravenous glucose tolerance test. The model is described by

$$\frac{dG}{dt} = - p_1 G(t) - X(t)(G(t) + G_b) + \frac{m(t)}{V_G} \quad (1)$$

$$\frac{dX}{dt} = - p_2 X(t) + p_3 I(t) \quad (2)$$

$$\frac{dI}{dt} = - n(I(t) + I_b) + U(t)/V_I \quad (3)$$

where $G(t)$ is the differential plasma glucose relative to the basal glucose value, G_b (mg/dl), X (unitless) is the insulin in the remote compartment, and I (mU/liter) is the differential plasma insulin relative to the basal insulin value, I_b. The volumes of gut and insulin distributions are V_G and V_I, respectively. The Bergman model parameters used for this study are p_1 = 1.0e-2 min^{-1}, p_2 = 3.33e-2 mU liter^{-1} min^{-2}, and p_3 = 1.33e-5 min^{-1}.[18] Model inputs are the plasma glucose appearance rate, $m(t)$, and the plasma insulin appearance rate, $U(t)$, a modification for T1DM in which insulin appears only from an exogenous source.[19]

The Bergman model describes the dynamics of insulin and glucose where the inputs are appearance rates into the bloodstream. For control applications and practical estimation of input values, an additional meal submodel is used to describe meal dynamics. Hovorka and coworkers[11] used the meal submodel described by a second-order process model:

$$U_G(t) = \frac{D_G A_G t e^{-t/t_{max,G}}}{t^2_{max,G}} \quad (4)$$

where D_G is the meal carbohydrate load (mg), A_G is the carbohydrate bioavailability, and $t_{max,G}$ (min^{-1}) is the time-of-maximum appearance rate of glucose in the accessible glucose compartment. The meal submodel can be expressed as a two-compartment gut absorption model

$$\frac{dm}{dt} = - \frac{1}{t_{max,G}} m(t) + \left(\frac{1}{t_{max,G}}\right) g(t) \quad (5)$$

$$\frac{dg}{dt} = - \frac{1}{t_{max,G}} g(t) + \left(\frac{A_G}{t_{max,G}}\right) D_G(t) \quad (6)$$

where $g(t)$ is the glucose appearance in the first compartment and $m(t)$ (mg) is the plasma appearance of glucose, an input for the Bergman model.

There is also the need to incorporate the subcutaneous insulin kinetics into the model. The model used to describe the subcutaneous insulin transport to plasma insulin was reported by Hovorka *et al.*[11] as a two-compartment insulin absorption model:

$$\frac{dS_2}{dt} = - \frac{S_1(t)}{t_{max,I}} - \frac{S_2(t)}{t_{max,I}} \quad (7)$$

$$\frac{dS_1}{dt} = - u(t) - \frac{S_1(t)}{t_{max,I}} \quad (8)$$

where S_1 is the amount of insulin in the first compartment, S_2 is the amount of insulin in the second compartment, $t_{max,I}$ is the time to maximum of absorption of subcutaneously injected insulin, and $u(t)$ is the administration of insulin, which can be either bolus or basal infusion.[8] The plasma insulin appearance rate that appears as an input in **Equation (1)** of the Bergman model, $U(t)$, is represented by

$$U(t) = S_2(t)/t_{max,I} . \quad (9)$$

For *in silico* testing, the full model of Hovorka *et al.*[11] is used to describe the glucose–insulin dynamics of a T1DM subject. The physiological model, which describes the glucoregulatory network, incorporates a two-compartment glucose subsystem, an insulin subsystem, and a three-compartment insulin action subsystem.

State Estimation

The KF is a state estimator used to estimate state variables that cannot be measured directly. It is based on a linear discrete state space model,

$$x_{k+1} = \Phi x_k + \Gamma u_k + \Gamma^w w_k \quad (10)$$

$$y_k = C x_k + \Gamma^v v_k \quad (11)$$

where x (nx1) is the state vector of n state variables, the input vector, u (n_ux1), has n_u inputs, Φ (nxn), C (n_yxn), Γ (nxn_u), Γ^w (nx1), and Γ^v (n_yx1) are consistent matrices, and k is the time index. The measured output, y (n_yx1), is the output vector of n_y measurements. In this research, process noise, w_k, and measurement noise, v_k, are assumed to be scalars with zero means and variances denoted by

$$\text{var}(w) = Q \quad (12)$$

$$\text{var}(v) = R \quad (13)$$

Because Q and R are not measurable, they are considered to be tuning parameters. The ratio of Q/R is adjusted as a tuning parameter, reflecting the trade-off between trusting the measurement and trusting the model prediction. A large Q/R ratio is used when confidence

is placed on the measurement, and a small Q/R ratio is applied when the measurement noise is high, the model is accurate, and thus is trusted more.

The KF algorithm is illustrated in **Figure 1** where $\hat{x}_{k|k-1}$ is the state estimate at time k based on information at time $k-1$, i.e., the one-step ahead prediction, L_k is the Kalman gain, P_k is the state covariance, and I is the identity matrix. The state estimate is based on the model:

$$\hat{x}_{k|k-1} = \Phi\hat{x}_{k-1|k-1} + \Gamma u_{k-1} \quad (14)$$

$$\hat{y}_{k|k-1} = C\hat{x}_{k|k-1} \quad (15)$$

where $\hat{y}_{k|k-1}$ is the predicted output at time k. The corrected estimate of the state vector, $\hat{x}_{k|k}$, is obtained by updating using the current measurement, y_k, and the Kalman gain, L_k,

$$\hat{x}_{k|k} = \hat{x}_{k|k-1} + L_k(y_k - C\hat{x}_{k|k-1}) \quad (16)$$

Model Predictive Control

The control actions determined by MPC are calculated by minimizing the objective function,

$$\min_{\Delta u} J = \hat{E}^T W^y \hat{E} + \Delta u^T W^u \Delta u \quad (17)$$

and the error is calculated over the prediction horizon, P:

$$\hat{E} = (r - \hat{y}_{k+i|k}) \quad (18)$$

where r is the set point, $\hat{y}$ is the vector of predicted outputs, and the superscript T denotes transpose of the matrices.[21] Because all state variables are not measurable, the KF is used to estimate the current model state across P. The change in manipulated input from one sample time to the next is Δu, which is evaluated over the control move horizon, and M, W^y, and W^u are diagonal matrices with identical elements equal to w^y and w^u, respectively. For MPC applications, the first control move, Δu_k, is implemented and the optimization is repeated at the next time step.

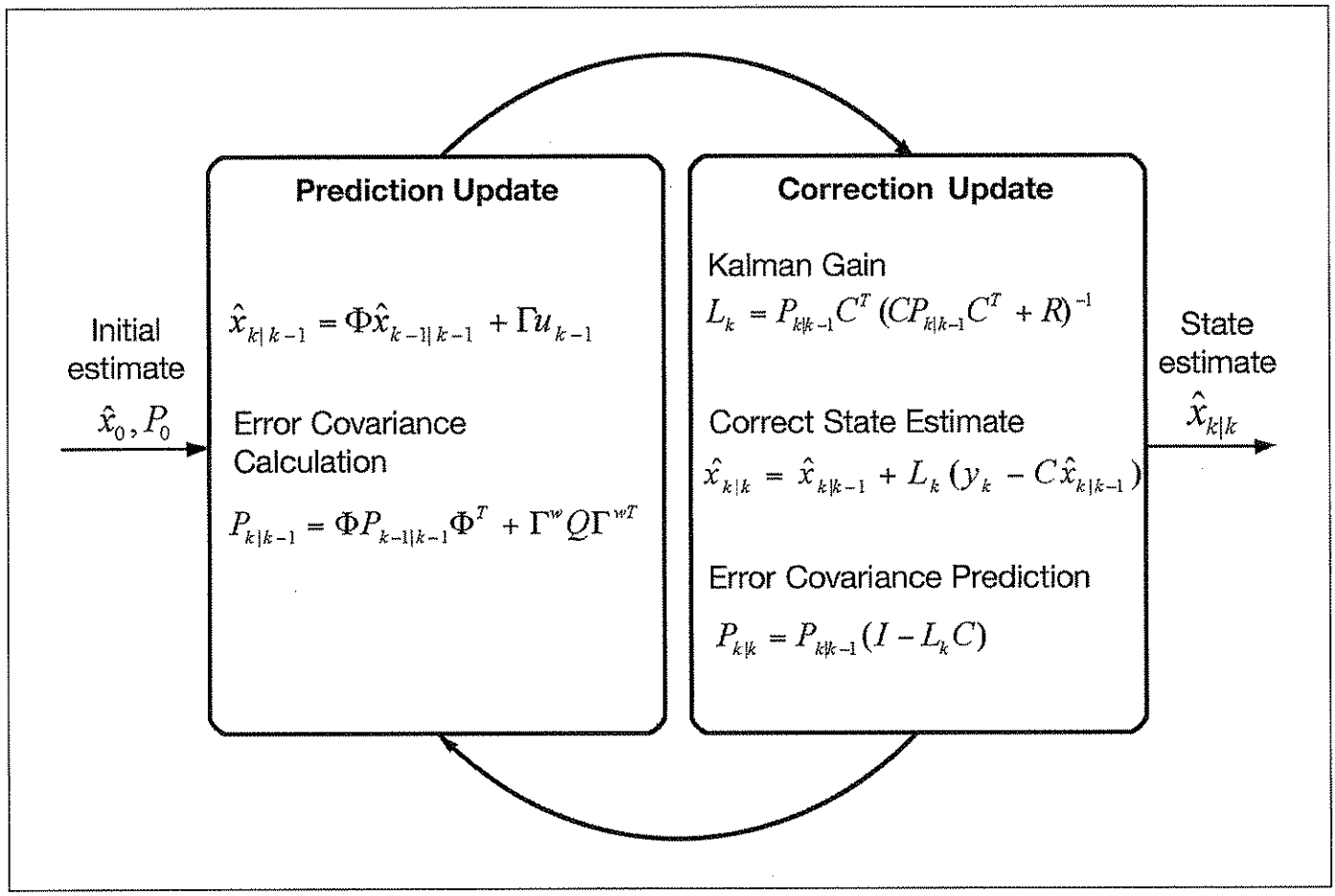

Figure 1. The recursive Kalman filter, which uses the previous estimated state, $x_{k|k-1}$, and current measurement, y_k, to calculate the estimate of the current state based on the error covariance, P_k.[20]

Advisory mode MPC is used to calculate control moves based on historical data in order to test the validity of the control system. This method is described by Seborg *et al.*[22] as a step in the implementation of MPC, referred to as "prediction mode." Because the control moves calculated for advisory mode have no causal impact on historical data, the moves are analyzed on a time-step by time-step basis. For diabetes control, the advisory moves are compared to insulin recommendations made by physicians for the conditions of the historical data set. **Figure 2** compares the information provided to the controller at a single time step and the recommended MPC insulin move for actual glucose and insulin infusion data. Because this insulin recommendation is not implemented, the information provided to the controller at the next time step only includes insulin and glucose from the historical data set.

Data Collection

Data were collected from three adult subjects with T1DM [two females, one male; age: 45 ± 18 years (mean ± standard deviation); body mass index: 20.9 ± 1.7 kg/m^2; weight: 61 ± 7 kg; glycosylated hemoglobin A1c: 6.8 ± 1.3%] wearing continuous glucose sensors (CGMS®, Medtronic MiniMed, Inc., Northridge, CA). Five-minute glucose sampling produced 288 measurements per day for a total of 26 days. Insulin infusion information was retrieved from the insulin pump after the test period. Meal size estimates, exercise, and stress data were logged in a diary by subjects. Data sets that included saturation at the upper (400 mg/dl) or lower (40 mg/dl) limit of the CGMS for more than 12 consecutive samples were discarded from the analysis. Ninety-seven meal responses over 20 days of data were analyzed for the three subjects: 8 days with 42 meals for subject 1, 8 days with 29 meals for subject 2, and 4 days with 26 meals for subject 3.

Table 1.
Maximum Model Prediction Horizons for Each Subject (Mean ± Standard Deviation)

		Subject 1[1] (min)	Subject 2[1] (min)	Subject 3[2] (min)
with meal estimate	constant model	33 ± 12	48 ± 16	44 ± 19
	adaptation through $\hat{p}_i$	36 ± 9	45 ± 23	43 ± 25
no meal estimate	constant model	33 ± 14	34 ± 11	40 ± 13
	adaptation through $\hat{p}_i$	45 ± 12	48 ± 17	45 ± 28
	adaptation through $\hat{d}$	43 ± 13	49 ± 16	44 ± 30

[1]Based on 8 days of subject data.
[2]Based on 4 days of subject data.

Results

A KF based on the linearized Bergman minimal model with online model adaptation was used for glucose estimation and extended for application in MPC. State estimation and MPC were initially validated on the Hovorka model. These methods were then applied to historical subject data.

Simulation Study

Plant-model mismatch, similar to the ones considered by Lynch and Bequette,[10] was used to test the estimation capability of the KF *in silico*. To simulate a subject with T1DM, the Hovorka model was used to produce glucose values for a meal response with 10% Gaussian noise on

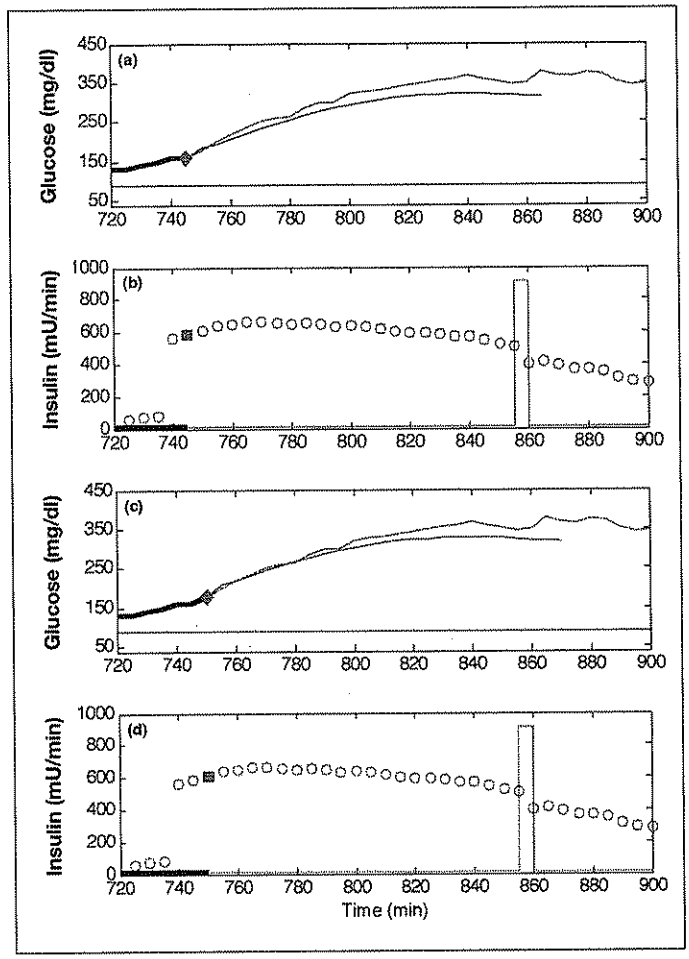

Figure 2. Two advisory mode MPC recommendations for the insulin infusion rate. They were calculated at the times denoted by diamonds: t = 745 minutes (a and b) and t = 750 minutes (c and d). Each G plot compares clinical glucose data (solid line) with the predicted trajectory (dot–dash line) and the desired value of 80 mg/dl (dashed line). Actual insulin infusion rates are denoted by hollow squares, whereas the two advisory mode recommendations are shown as solid squares. At t = 735 minutes, a 57-gram carbohydrate meal was ingested. The correction insulin bolus at approximately t = 855 minutes is shown as a rectangular pulse.

the measurements, which is in the expected range for the physical system. The linearized Bergman-based KF with $Q/R = 0.1$ was validated on meal response data in **Figure 3**. The state vector for the Bergman model is $x^T = [G; X; I; S_1; S_2; g; m]$, where the initial steady-state condition for linearization is $x_0^T = [81; -2.7e\text{-}3; -1.13; 0; 0; 0; 0]$ for a basal insulin infusion rate of 4.25 mU/min. Estimated glucose values were very close to those generated by the open-loop meal response of the Hovorka model, showing only minor mismatch at the onset of the meal response. The maximum glucose excursion was reduced from G_{max} = 260 mg/dl to G_{max} = 115 mg/dl, and an improvement in the settling time from $t_s > 1000$ minutes to $t_s < 300$ minutes was accomplished using MPC (**Figure 4**). The MPC tuning parameters were $P = 12$, $M = 3$, and $w^u/w^y = 0.001$.

Experimental Study

Glucose estimation and prediction obtained from a KF were applied to historical data for ambulatory conditions

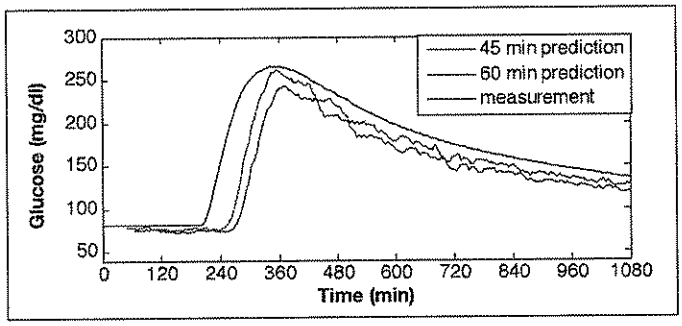

Figure 3. Glucose predictions using a constant model Kalman filter with no meal information for a 50-gram carbohydrate meal at $t = 200$ minutes and prediction horizons of 45 and 60 minutes ($Q/R = 0.1$).

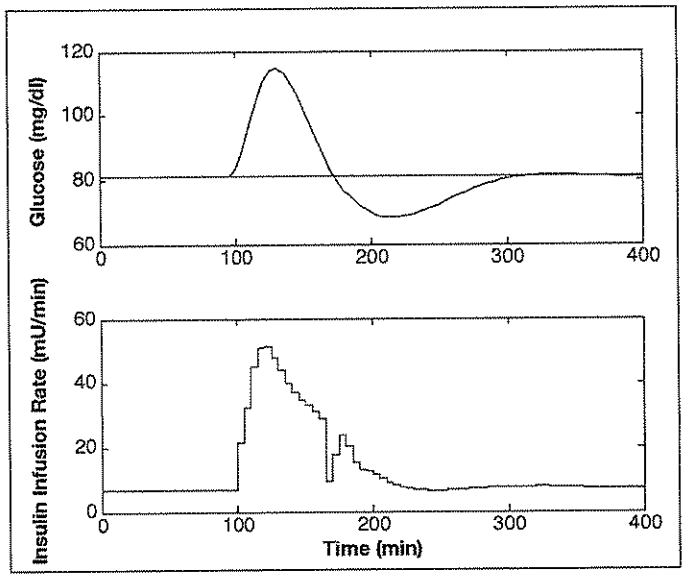

Figure 4. Model predictive control with state estimation based on linearized Bergman model with constant parameter values and insulin infusion rates for a 50-mg CHO meal at $t = 100$ minutes and $P = 12$, $M = 3$, and $w^u/w^y = 0.001$.

to determine the maximum number of steps ahead that glucose values can be accurately predicted by the model (i.e., *the maximum prediction horizon*). It was determined using qualitative analysis of the fit of the prediction as well as the evaluation of the *median relative absolute difference* (MRAD). The MRAD is calculated as

$$MRAD = median\left[\left(\frac{|\hat{y}_k - y_k|}{y_k}\right)\right] \times 100\% \qquad (19)$$

The threshold for maximum model prediction for the 24-hour period was specified in this study as MRAD ≤ 16%. Maximizing the prediction horizon is essential for the successful application of advanced control strategies.

The KF was first evaluated with meal estimates for the estimator based on the linearized Bergman model, modified to include gut absorption and subcutaneous insulin processing models with $Q/R = 10$. In **Figure 5**, 45-, 60-, and 90-minute-ahead glucose predictions show the limits in the prediction capability of the model for subject 2, day 6. The KF is able to predict the glucose levels of these ambulatory subject data through meal responses and subcutaneous insulin boluses, while exhibiting only slight subject-model mismatch for the smaller prediction horizons (45 or 60 minutes), but as the horizon is increased to 90 minutes, the prediction is less accurate. Maximum prediction horizons for the multiple data sets (mean ± standard deviation) are 33 ± 12 minutes for subject 1, 48 ±16 minutes for subject 2, and 44 ± 19 minutes for subject 3.

Ideally, an artificial pancreatic β cell should remove the subject entirely from the closed-loop system, which

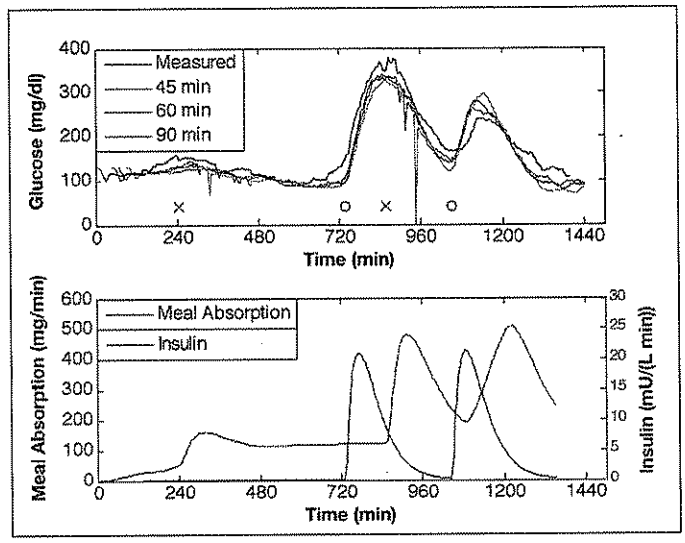

Figure 5. Glucose predictions for prediction horizons of 45, 60, and 90 minutes ahead based on KF state estimation with $Q/R = 10$ and meal estimate provided. Meal time is denoted by "o" and insulin bolus time by "x" (top plot).

requires the model and estimator to predict glucose accurately with no meal information. **Figure 6** illustrates the KF glucose predictions for horizons of 45 and 60 minutes based on the modified, linear Bergman model (Q/R = 10). With no meal information provided to the model, the prediction exhibits no input-driven glucose response. Maximum prediction horizons are 33 ± 14, 34 ± 11, and 40 ± 13 minutes for subjects 1, 2, and 3, respectively.

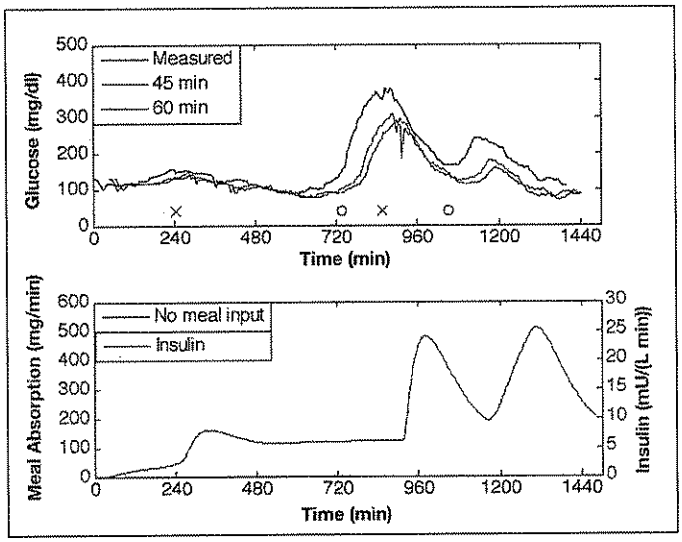

Figure 6. Glucose predictions for prediction horizons of 45 and 60 minutes based on KF state estimation with Q/R = 10 and no meal estimate provided. Meal time is denoted by "o" and insulin bolus time by "x" (top plot).

Model adaptation was introduced to compensate for subject-model mismatch and the lack of meal information. Two approaches were taken to allow online adaptation of the modified Bergman model. First, **Equation (1)** was revised with the augmentation and estimation of $\hat{p}$ in the form:

$$\frac{dG}{dt} = -\hat{p}_1(t)G(t) - X(t)(G(t) + G_b) + \frac{m(t)}{V_G} \quad (20)$$

$$\frac{d\hat{p}_1}{dt} = 0, \quad (21)$$

which was linearized for use in the Kalman filter. Adaptation of $\hat{p}_1$ improves the prediction ability for input responses with no meal information given, as demonstrated in **Figure 7** ($Q/R = 10^{-2}$). The negative excursion in $\hat{p}_1$ during a meal response to simulate glucose production allows the model to respond to the glucose peak; maximum prediction horizons are improved to 45 ± 12 minutes for subject 1, 48 ± 17 minutes for subject 2, and 45 ± 28 minutes for subject 3.

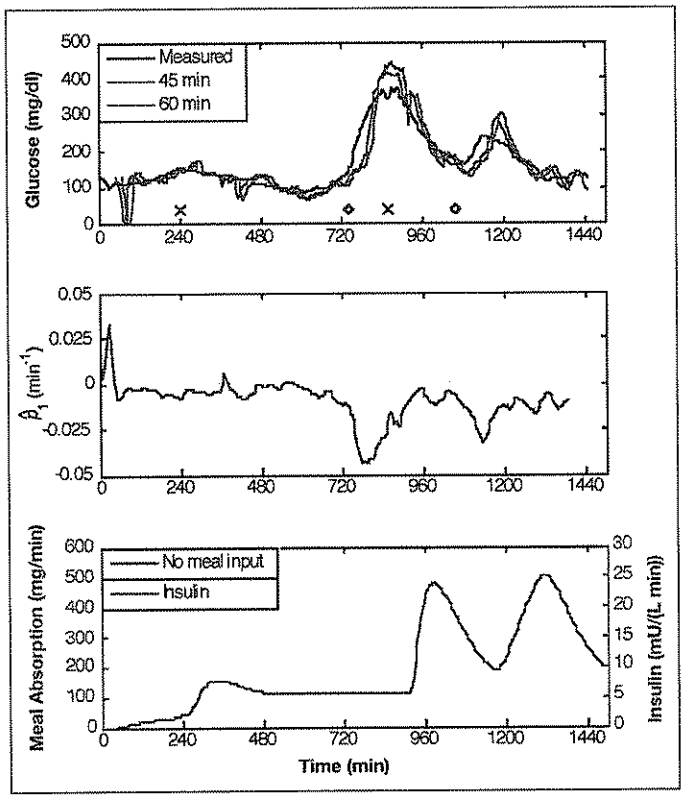

Figure 7. Glucose predictions for prediction horizons of 45 and 60 minutes based on KF state estimation with $\hat{p}_1$ adaptation, $Q/R = 10^{-2}$, and no meal information provided. Meal time is denoted by "o" and insulin bolus time by "x" (top plot).

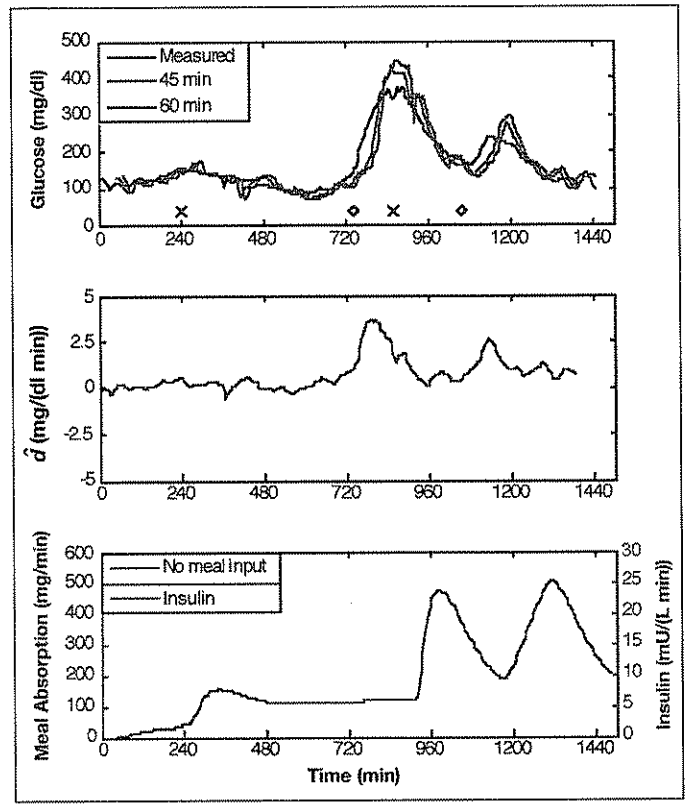

Figure 8. Glucose predictions for prediction horizons of 45 and 60 minutes based on KF state estimation with $\hat{d}$ adaptation, Q/R = 10-4, and no meal information provided. Meal time is denoted by "o" and insulin bolus time by "x" (top plot).

An alternative approach incorporates an additive disturbance term, $\hat{d}$, for adaptation of **Equation (1)** in the form:

$$\frac{dG}{dt} = -\ p_1 G(t) - X(t)(G(t) + G_b) + \frac{m(t)}{V_G} + \hat{d}(t) \qquad (22)$$

$$\frac{d(\hat{d})}{dt} = 0, \qquad (23)$$

Because adaptation of either $\hat{d}$ or $\hat{p}_1$ has an indirect effect on $G(t)$, the prediction capability for either type of model adaptation is similar, as shown in **Figures 7** and **8**. **Figure 8** presents model predictions for $\hat{d}$ adaptation and $Q/R = 10^{-4}$. The maximum prediction horizons are 43 ± 13, 49 ± 16, and 44 ± 30 minutes for subjects 1, 2, and 3, respectively.

A prediction horizon of 60 minutes was implemented in an advisory mode MPC scheme, with KF state estimation, to evaluate the controller action based on retrospective subject data. The controller was tuned to generate moderately aggressive control moves in response to meal excursions. Advisory moves from MPC with $P = 12$, $M = 3$, and $w^u/w^y = 0.1$ with the KF based on a constant model with meal estimates given and $Q/R = 10$ are reported in **Figure 9** for subject 2, day 6. The controller recommends significant increases in insulin at the moments that the meals were reported to have begun ($t = 735$ minutes and $t = 1050$ minutes), which resulted from the meal estimates. This response preceded the insulin action from a late meal bolus reported by the subject. Insulin recommendations from MPC with the same controller tuning and subject data are reported in **Figure 10** for conditions when the MPC received no meal information. The KF was based on $\hat{d}$ adaptation with $Q/R = 0.005$. Although the calculated MPC insulin action did not change at the exact moment that the first meal was reported, the increased insulin recommendation led the actual insulin bolus. By responding early to the onset of the meal, the glucose excursion could probably be reduced using MPC.

Conclusions and Future Work

Glucose estimation and prediction for T1DM subject data were accomplished using a KF based on a linearized version of a modified Bergman model. Maximum prediction horizons were determined for 20 days of ambulatory subject data. With meal estimates provided,

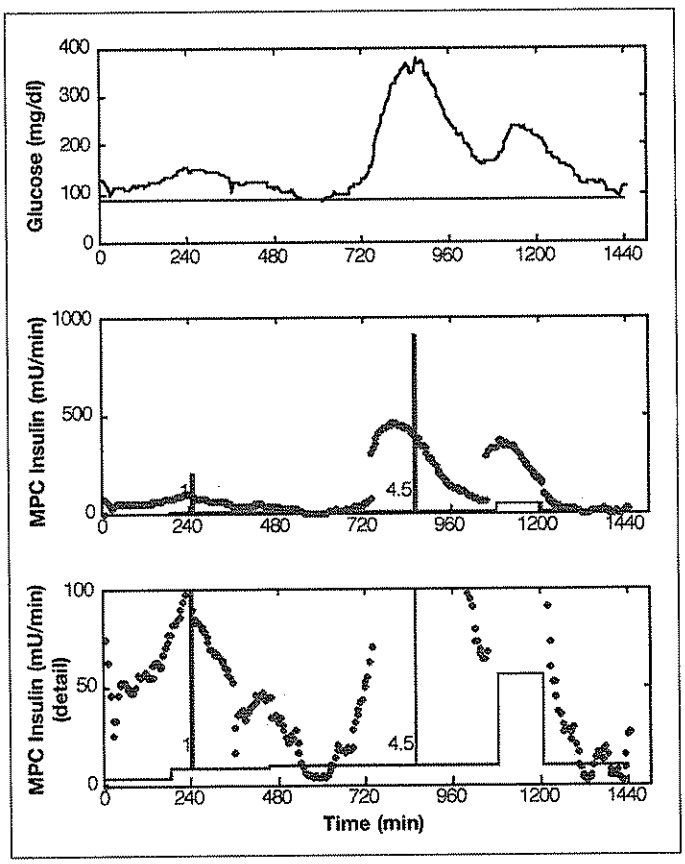

Figure 9. Results for measured meal disturbance (meals: $t = 735$ and $t = 1050$). Glucose levels and advisory mode MPC recommendations $Q/R = 10$, $P = 12$, $M = 3$, and $w^u/w^y = 0.1$.

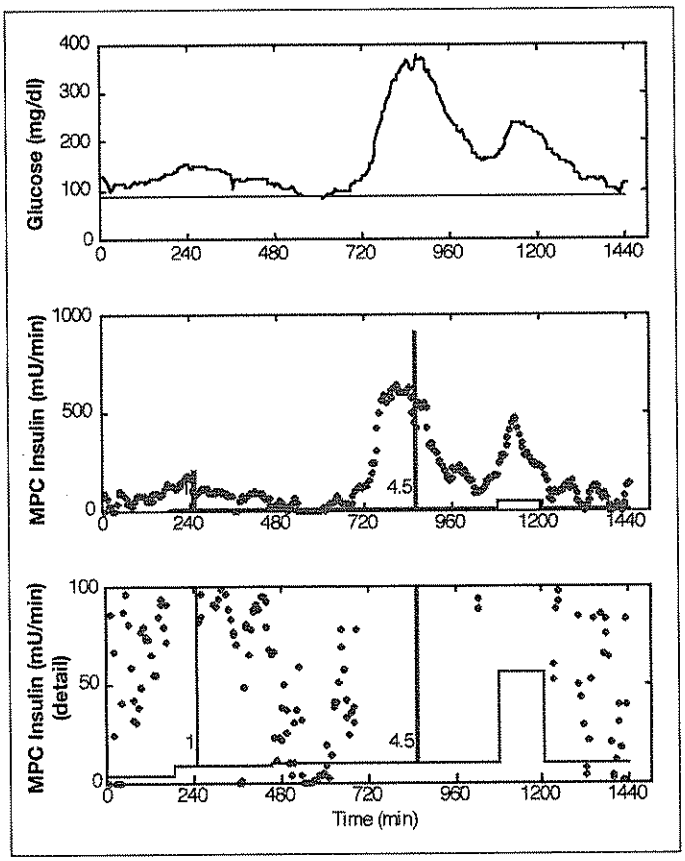

Figure 10. Results for unmeasured meal disturbance (meals: $t = 735$ and $t = 1050$). Glucose levels and advisory mode MPC recommendations $Q/R = 0.005$, $P = 12$, $M = 3$, and $w^u/w^y = 0.1$.

the constant model adequately predicted the glucose levels through meal information with a maximum prediction horizon of 48 minutes. By incorporating model parameter adaptation, comparable prediction horizons were obtained when no meal information was available. Results of the advisory mode MPC indicate that this control strategy could improve glucose control through the meal response in subjects with T1DM. This was demonstrated with advisory MPC insulin in response to the rising glucose levels prior to the late insulin boluses for the meals.

Future studies will include clinical implementation of MPC to control glucose levels through the entire meal responses. This control method will be validated for both "normal" and days with abnormal insulin sensitivities due to exercise or stress.

Funding:

Juvenile Diabetes Research Foundation and National Institutes of Health Grants R01-DK068706-02, R01-DK068663-02, and R21-DK069833-01.

Disclosures:

This research was conducted in part with support from the Investigator-Initiated Study Program of LifeScan, Inc. We also thank Medtronic MiniMed, Inc. for their generous support.

References:

1. Geiss LS, Herman WH, Smith PJ. Mortality in non-insulin-dependent diabetes. National Diabetes Data Group, editors. Diabetes in America. 2nd ed. Washington, DC: U.S. Department of Health and Human Services, National Institutes of Health, National Institute of Diabetes and Digestive and Kidney Diseases. NIH Publication No. 95-1468;1995:233-57.
2. Geiss LS, Rolka DB, Engelgau MM. Elevated blood pressure among U.S. adults with diabetes, 1988-1994. Am J Prev Med. 2002;22(1):42-9.
3. Klein R, Klein BE. Vision disorders in diabetes. National Diabetes Data Group, editors. Diabetes in America. 2nd ed. Washington, DC: U.S. Department of Health and Human Services, National Institutes of Health, National Institute of Diabetes and Digestive and Kidney Diseases. NIH Publication No. 95-1468;1995:293-336.
4. The Diabetes Control and Complications Trial Research Group. The effect of intensive treatment of diabetes on the development and progression of long-term complications in insulin-dependent diabetes mellitus. N Engl J Med. 1993;329:977-86.
5. Centers for Disease Control and Prevention. National diabetes fact sheet: general information and national estimates on diabetes in the United States, 2005. Atlanta GA: U.S. Department of Health and Human Services, Centers for Disease Control and Prevention; 2005.
6. Parker RS, Doyle FJ III, Peppas NA. The intravenous route to blood glucose control. IEEE Trans Biomed Eng. 2001;20(1):65-73.
7. Parker RS, Doyle FJ III, Peppas NA. A model-based algorithm for blood glucose control in type I diabetic patients. IEEE Trans Biomed Eng. 1999;46(2):148-57.
8. Parker RS, Gatzke EP, Doyle FJ III. Advanced model predictive control (MPC) for type I diabetic patient blood glucose control. Proc Am Contr Conf. 2000;3483-7.
9. Kuure-Kinsey M, Palerm CC, Bequette BW. A dual-rate Kalman filter for continuous glucose monitoring. Proceedings of the 28th IEEE EMBS Annual International Conference; 2006.
10. Lynch SM, Bequette BW. Model predictive control of blood glucose in type I diabetics using subcutaneous glucose measurements. Proc Am Contr Conf. 2002;4039-43.
11. Hovorka R, Canonico V, Chassin LJ, Haueter U, Massi-Benedetti M, Federici MO, Pieber TR, Schaller HC, Schaupp L, Vering T, Wilinska ME. Nonlinear model predictive control of glucose concentration in subjects with type 1 diabetes. Physiol Meas. 2004;25(4):905-20.
12. Sorensen JT. A physiologic model of glucose metabolism in man and its use to design and assess improved insulin therapies for diabetes [thesis]. Cambridge: MIT; 1985.
13. Bergman RN, Ider YZ, Bowden CR, Cobelli C. Quantitative estimation of insulin sensitivity. Am J Physiol Endocrinol Metab Gastrointest Physiol. 1979;236(6), E667-77.
14. Cobelli C, Federspil G, Pacini C, Salvan A, Scandellari C. An integrated mathematical model of the dynamics of blood glucose and its hormonal control. Math Biosci. 1982;58:27-60.
15. Cobelli C, Mari A. Validation of mathematical models of complex endocrine–metabolic systems. A case study on a model of glucose regulation. Med Biol Eng Comput. 1983;21:390-9.
16. Hovorka R, Shojaee-Moradie F, Carroll PV, Chassin LJ, Gowrie IJ, Jackson NC, Tudor RS, Umpleby AM, Jones RH. Partitioning glucose distribution/transport, disposal, and endogenous production during IVGTT. Am J Physiol Endocrinol Metab. 2002;282(5):992-1007.
17. Makroglou A, Li J, Kuang Y. Mathematical models and software tools for the glucose-insulin regulatory system and diabetes: an overview. Appl Num Math. 2006;56(3-4):559-73.
18. Owens CL. Control of blood glucose concentration for people with type 1 diabetes mellitus [thesis]. Newark (DE): University of Delaware; 2004.
19. Ollerton RL. Application of optimal control theory to diabetes mellitus. Int J Control. 1989;50(6):2503-22.
20. Welch G, Bishop G. An introduction to the Kalman filter. SIGGRAPH 2001 course 8. In Computer Graphics, Annual Conference on Computer Graphics & Interactive Techniques; 2001 Aug 12-17. Los Angeles: ACM Press, Addison-Wesley SIGGRAPH 2001 course pack edition.
21. Bequette BW. Process control: modeling, design, and simulation. Upper Saddle River (NJ): Prentice Hall; 2003.
22. Seborg DE, Edgar TF, Mellichamp DA. Process Dynamics and Control. 2nd ed. Hoboken (NJ): John Wiley & Sons, Inc.; 2004.